

The Functional Role of Hippocampal Subregions and Subfields:
A High-Resolution fMRI Study of Memory

by

Melanie Carol MacGillivray

A thesis submitted in partial fulfillment of the requirements for the degree of

Master of Science

Neuroscience & Mental Health Institute
University of Alberta

© Melanie Carol MacGillivray, 2017

Abstract

The involvement of the hippocampus in episodic memory is well accepted. What is often overlooked is the involvement of hippocampal subfields and subregions. The hippocampal subfields Cornu Ammonis (CA), Dentate Gyrus (DG) and Subiculum (Sub) are cellularly distinct areas that communicate transversely across the hippocampus, while hippocampal subregions (Head, Body & Tail) are delineated from anterior to posterior along the length of the hippocampus and have different cortical connectivity.

The current study addressed the question of how hippocampal subfields and subregions are involved in the encoding of episodic memory using high-resolution fMRI and an adaptation of the Wechsler Memory Scale Designs Subtest (2009). Our memory tasks consisted of 3 conditions: Symbol (content memory), Location (spatial memory) and Both (associative memory).

We found that the total hippocampus was active for the Symbol, Location and Both conditions. All subfields and subregions were active across all conditions of the task relative to baseline. DG activity was significantly larger than CA activity when averaged across conditions. For the Location condition the hippocampal tail was more active than the hippocampal body, suggesting it may play a more dominant role in spatial memory. In addition hemisphere by subfield and subfield by condition interactions were observed.

Our results provide support for the theory of posterior hippocampal involvement in spatial memory, and suggest the human hippocampus works in discrete but connected subsections to encode episodic memory.

Acknowledgements

I would like to thank my supervisor Dr. Nikolai Malykhin, for the opportunity to participate in such an exciting and innovative research project. Thank you for guiding me throughout the project, having patience and always being there to keep everything moving forward.

A special thanks goes to Stanislaw Hrybowski for teaching me all about fMRI and the process of good science. He has guided me throughout the project and I am grateful for his mentorship. I would also like to thank the contributors to our project. Chris Madan for his help with task design and fMRI analysis, Peter Seres for his many hours of work and patience setting up and running participants for the project, Yushan Huang for all his hard work and many hours spent tracing hippocampi and making this project possible and Rawle Carter for his work on recruitment, screening and scheduling of participants for the study.

I would also like to thank my committee members Jacqueline Cummine and Jeremy Caplan for their feedback and guidance throughout this project. And thank you to my lab mates Arash Sereshki and Scott Travis for being great anchors and sources of support throughout graduate school and research project progression.

Lastly, I would also like to thank my parents and Sam Worrall for being great support systems throughout my degree and encouraging me to pursue this degree program and my dreams. This research was funded by Canadian Institutes of Health Research (CIHR) operating grants (PI – Nikolai Malykhin). The results have been presented in part at the Society for Neuroscience Annual Meeting 2016 in November in San Diego, California, USA, Campus Alberta Neuroscience International Banff Conference 2016 and Organization for Human Brain Mapping (OHBM) annual meeting in Vancouver, British Columbia, Canada, in June 2017.

Table of Contents

Chapter 1: Introduction	1
1.1: Introduction to Memory in the Hippocampus.....	1
1.2: Hippocampal Anatomy	3
1.3: Hippocampal Subfields and Subregions in Memory Function	13
1.4: Models of Hippocampal Function.....	16
1.5: Objective	18
Chapter 2: Material & Methods	19
2.1: Participants.....	19
2.2: Stimuli.....	19
2.3: Memory Task	20
2.4: Experimental Design.....	25
2.5: Data Acquisition	25
2.6: Hippocampal Segmentation	27
2.7: Image Preprocessing	28
2.8 General Linear Model and HRF Fitting.....	30
2.9: Imaging Analysis	32
Chapter 3: Results	35
3.1: Behavioural Results	35
3.2: Total Hippocampus.....	36
3.3: Subregions.....	38
3.4: Subfields.....	41
Chapter 4: Discussion	46
4.1: Comparison Canonical & Canonical + Derivative Results.....	47
4.2: Models of Hippocampal Structure & Function.....	51

4.3: Encoding	54
4.4: Spatial Memory.....	55
4.5: Limitations & Future Directions	57
4.6: Summary	58
References	60

List of Figures

1.1: Sagittal MRI Image Showing the Location of the Hippocampus in the Human Brain	3
1.2: Coronal Histological Slice Showing Hippocampal Subfields	4
1.3: Coronal MRI Images Delineating Subfields within Subregions	5
1.4: Comparison of Typical and High-Resolution fMRI	6
1.5: Visual Representation of the Direct Intrahippocampal Pathway	7
1.6: Visual Representation of the Polysynaptic Pathway	8
1.7: Visual Representation of the Polysynaptic Pathway Cortical Connections	8
1.8: MRI and 3-D Images Showing the Hippocampal Head, Body and Tail	9
1.9: Cross-species Comparison of Hippocampal Anatomy	10
1.10: Model of Long-Axis Specialization & Cortical Connectivity	12
1.11: Sensory Input onto the Long-Axis of the Hippocampus	12
1.12: Models of Hippocampal Functional Organization	17
2.1: Visual Depiction of Study Stimuli	20
2.2: Visual Depiction of the Symbol Condition	22
2.3: Visual Depiction of the Location Condition	22
2.4: Visual Depiction of the Both Condition with Location Cues	23
2.5: Visual Depiction of the Both Condition with Symbol Cues	23
2.6: Brain coverage in anatomical and functional scans	26
2.7: Hippocampal subfield ROIs shown on structural and functional images	28
2.8: Total Hippocampal HRF fitted to Canonical Modelling	31
2.9: Total Hippocampal HRF fitted to Canonical + Derivative Modelling	32
3.1: Behavioural Accuracy	35
3.2: Activation for Total Hippocampus (Canonical Modelling)	37
3.3: Activation for Total Hippocampus (Canonical + Derivative Modelling)	37

3.4: Activation for Subregions (Canonical Modelling)	39
3.5: Activation for Subregions (Canonical + Derivative Modelling)	40
3.6: Activation for Subfields (Canonical Modelling): Main Effect of Subfield	42
3.7: Activation for Subfields (Canonical Modelling): Hemisphere by Subfield Interaction	43
3.8: Activation for Subfields (Canonical Modelling): Condition by Subfield Interaction	43
3.9: Activation for Subfields (Canonical Modelling)	45
3.10: Activation for Subfields (Canonical + Derivative Modelling)	45

List of Tables

4.1: Differences observed between Canonical and Canonical + Derivative Modelling	49-50
--	-------

List of Abbreviations

2-D	Two-Dimensional
3-D	Three-Dimensional
CA	Cornu Ammonis
DG	Dentate Gyrus
fMRI	Functional Magnetic Resonance Imaging
FOV	Field of View
FWE	Family Wise Error
FSE	Fast Spin Echo
mm	Millimetre(s)
MPRAGE	Magnetic Prepared Rapid Acquisition Gradient Echo
MRI	Magnetic Resonance Imaging
ms	Millisecond(s)
MTL	Medial Temporal Lobe
PET	Positron Emission Tomography
SD	Standard Deviation
SE	Spin Echo
SNR	Signal to Noise Ratio
Sub	Subiculum
T	Tesla
T1	Longitudinal Relaxation Time
T2	Transverse Relaxation Time
TE	Echo Time
TR	Repetition Time
WMS	Wechsler Memory Scale

Chapter 1: Introduction

1.1: Introduction to Memory in the Hippocampus

Episodic memory is long-term memory for past events, and can contain contextual information about previous experiences (Squire & Zola-Morgan, 2015). It is well accepted that the hippocampus plays a role in episodic memory (Eichenbaum, 2001). The inability of patient H.M. (Scoville & Milner, 1957) and other patients with hippocampal lesions (Squire & Zola-Morgan, 2011) to successfully perform episodic memory tasks lends support for this theory.

It is important to note that there are many different types of memory. In the current study we investigate hippocampal involvement in episodic memory. Often, memory is divided into dichotomies. For instance, memory is often classified as either long-term or working memory. Long-term memory is the ability to remember information from the past that is not kept in mind via active rehearsal (Jeneson & Squire, 2011). It can be contrasted with working memory, which is when a limited amount of information is kept in mind or recalled after a short delay without significant distraction (Jeneson & Squire, 2011). Long-term memory is needed to access information that is not actively kept in mind.

Long-term memory can be divided into declarative and procedural memory. Declarative memory can be consciously recalled, and can include contextual information about a past event or factual knowledge. Procedural memory is an unconscious memory for skills that can help guide behaviour subconsciously (Squire & Zola-Morgan, 2015).

Declarative memory can also be described as associative as it involves linking parts together by spatial, temporal or other features. While declarative memory is classified as longterm memory, working memory studies by Mayes et al. (2007) and Piekema et al. (2009) have shown hippocampal

activity during memory tasks that require associations to be made, especially when those associations were cross-modal.

Declarative memory can be further subdivided into episodic and semantic memory. Episodic memory refers to memory for past events, and can contain contextual information about previous experiences while semantic memory is memory for factual information (Squire & Zola-Morgan, 2015). Semantic memory is not tied to an event while episodic memory is specific to a certain time or place. A unique feature of episodic memory is that it allows humans and animals to “mental time travel” back to earlier events and relive them (Tulving, 2002). Our study assesses hippocampal involvement in the encoding of episodic memory.

First evidence for hippocampal involvement in episodic memory came from research done with patient H.M. (Scoville & Milner, 1957). Patient Henry Molaison underwent a bilateral medial temporal lobe (MTL) resection to help relieve severe epilepsy, where the hippocampus, amygdala and surrounding structures were removed (Squire & Zola-Morgan, 2011). He was unable to form new episodic memories following the surgery, and lost all memory for years leading up to the surgery (Scoville & Milner, 1957). Following this discovery, there have been many studies comparing medial temporal lobe patients with healthy controls that imply the hippocampus as a whole plays a role in episodic memory. For instance, a study performed by Olson et al (2006) where patients with MTL damage completed a task where they were asked to remember a series of coloured blocks over a short delay. They performed as well as controls at the shortest delay for all 6 items, but when a longer delay was introduced they were unable to remember more than a few. Jensen & Squire (2011) argued that in this case, there was likely too much information to be actively rehearsed in

working memory, so participants had to access their long-term memory system to help them complete the task.

1.2: Hippocampal Anatomy

The hippocampus is a structure found in the medial temporal lobe (See Figure 1.1). Hippocampus is the Latin word for seahorse, and it was named in such a way because its outer structure as a whole resembles a seahorse. It is a heterogeneous structure and is often divided into anatomical subdivisions known as hippocampal subfields and subregions.

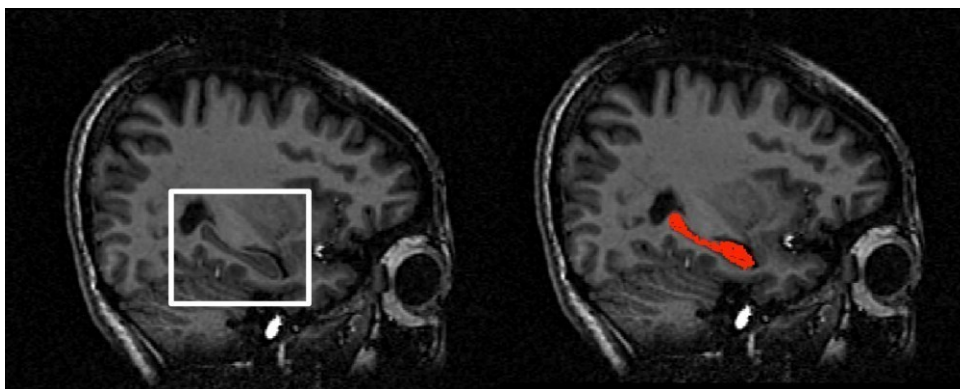


Figure 1.1: A sagittal MRI image showing the location of the hippocampus in the human brain.

Cross sectionally the hippocampus can be divided into cellularly distinct subfields known as the Cornu Ammonis (CA1-4), the Dentate Gyrus (DG) and the Subiculum (Sub) (Duvernoy, 2013). These subfields communicate transversely across the hippocampus and can be delineated on cross sectional post mortem images (See Figure 1.2 from Duvernoy, 2005) and visualized on coronal MRI images (See Figure 1.3 from Malykhin et al., 2010).

The CA subfield can be further divided into CA1-4 regions. This subfield is composed of pyramidal neurons with triangular soma in CA1 and ovoid soma in CA2-4. It is the largest subfield in the human hippocampus and takes up the majority of the outer perimeter (Duvernoy, 2013). The

DG is separated from the CA by the hippocampal sulcus and is located in the centre of the human hippocampus. It is composed of densely packed granular neurons (Duvernoy, 2013). The Sub is composed of pyramidal neurons and can be divided into the prosubiculum, subiculum proper, presubiculum and parasubiculum. The Sub is separated from the CA by the stratum radiatum and often referred to as the anatomical transition between the hippocampus and entorhinal cortex (Duvernoy, 2013).

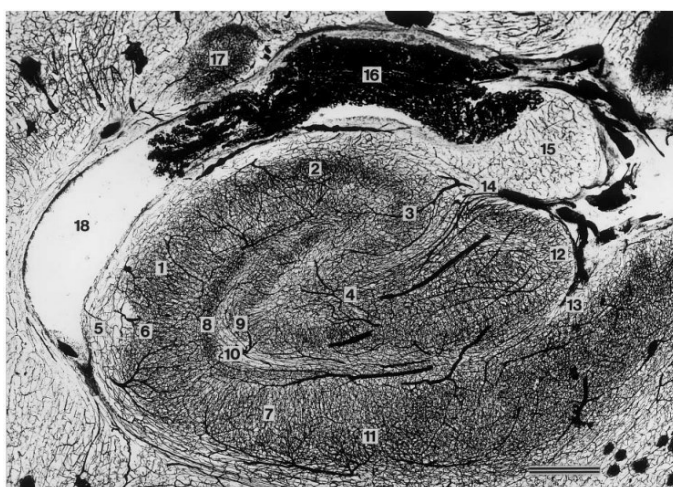


Figure 1.2: Coronal section of the hippocampal body after intravascular India ink injection. The layers of the hippocampus can be distinguished due to differences in their vascular density. The stratum moleculare of the cornu Ammonis (8) and that of the gyrus dentatus (9) are separated by the vestigial hippocampal sulcus (10). Note the high vascular density of the subiculum (11) in comparison to that of the adjacent stratum radiatum of CA1 (7), Bar, 1.5 mm
 Cornu Ammonis: 1–4, CA1 –CA4 (fields of the cornu Ammonis). Sublayers of CA1: 5, alveus; 6, stratum pyramidale; 7, strata radiatum and lacunosum; 8, stratum moleculare. Gyrus dentatus: 9, stratum moleculare; 10, vestigial hippocampal sulcus; 11, subiculum; 12, margo denticulatus; 13, superficial hippocampal sulcus; 14, fimbriodentate sulcus; 15, fimbria; 16, choroid plexuses; 17, tail of caudate nucleus; 18, temporal (inferior) horn of the lateral ventricle.

(Duvernoy, H.M., Cattin, F., Risold, P.Y. (2013). *The human hippocampus: Functional anatomy, vascularization, and serial sections with MRI*. Berlin Heidelberg: Springer-Verlag)

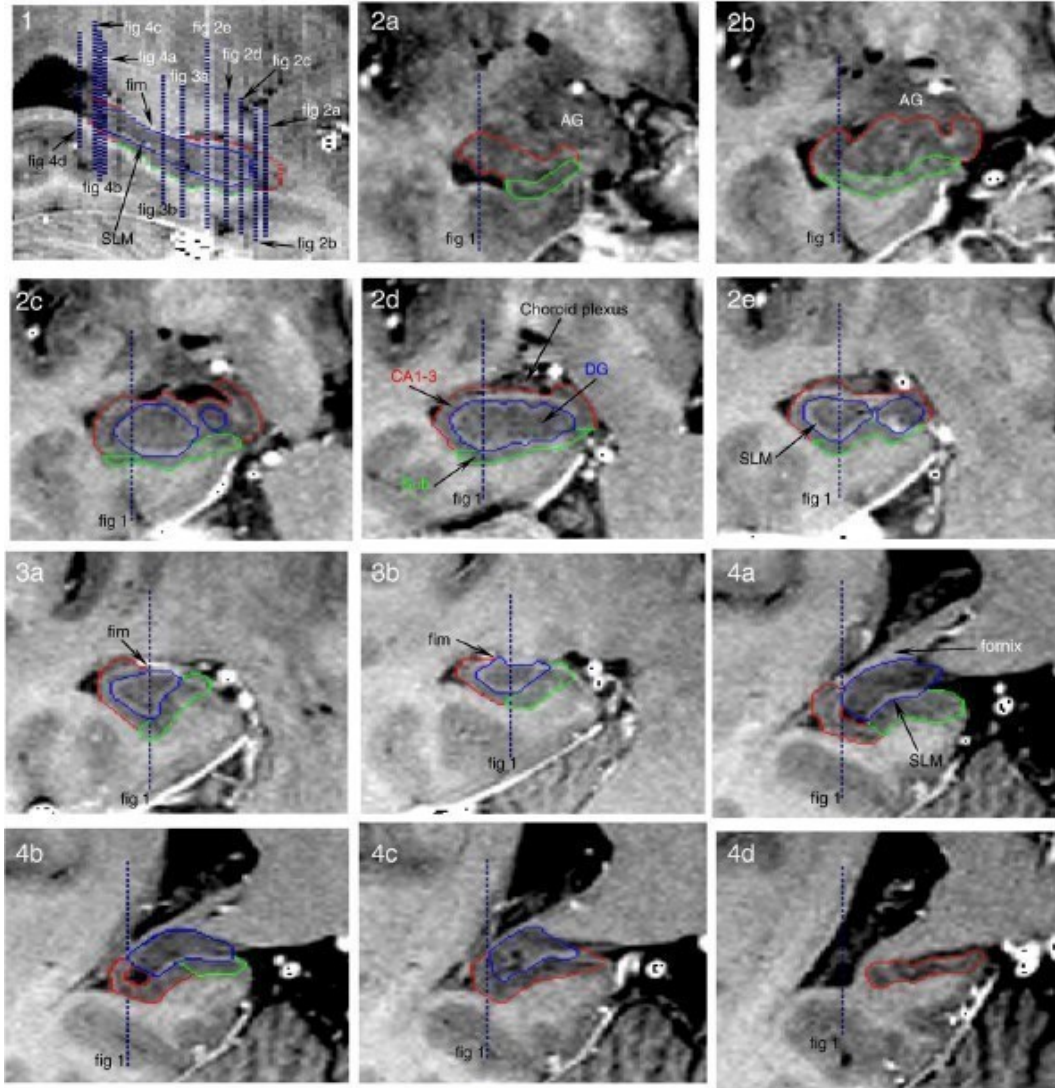


Figure 1.3: T2-weighted FSE images are shown in inverted contrast. Sagittal view of the hippocampus with references to coronal slices (1). Coronal views of the hippocampal parts (2–4): hippocampal head (Fig. 2d); hippocampal body (Fig. 3b); hippocampal tail (Fig. 4). Abbreviations: CA1-3, cornu ammonis (shown in red); DG, dentate gyrus (shown in blue); Sub, subiculum (shown in green); SLM, stratum lacunosum-moleculare; fim, fimbria. (Malykhin, N.V., Lebel, R.M., Coupland, N.J., Wilman, A.H., & Carter, R. (2010). In vivo quantification of hippocampal subfields using 4.7 T fast spin echo imaging. *Neuroimage*, 49,1224-30.)

Although there is some discrepancy in how to separate hippocampal subfields into more accurate anatomical Regions of Interest (ROIs) (Yushkevich et al., 2015), most studies segment the hippocampus into 3 main subfields: CA1-3, DG (+CA4) and Sub. The exact definition of the boundaries varies between more than 21 protocols for manual segmentation (Yushkevitch et al.,

2015). Using 3T most structural MRI studies are unable to delineate the border between the DG, CA3 and CA2 and therefore these regions are often combined to form an ROI known as DG/CA3 or DG/CA2/CA3 (Suthana et al., 2015). The current study divides these subfields into CA1-3, DG (+CA4) and Sub ROIs.

While typical fMRI voxels of 4 – 5 mm in plane are too coarse to measure activity across subfields that are only a few millimetres in width, high-resolution fMRI with voxels of less than 2 mm allows researchers to adequately investigate hippocampal subfield activity (See Duncan et al., 2014 ; Leal et al., 2014 ; Reagh et al., 2014 ; Suthana et al., 2015). Figure 1.4 illustrates the difference between typical and high-resolution acquisition, demonstrating the need for high-resolution data when studying hippocampal subfields.

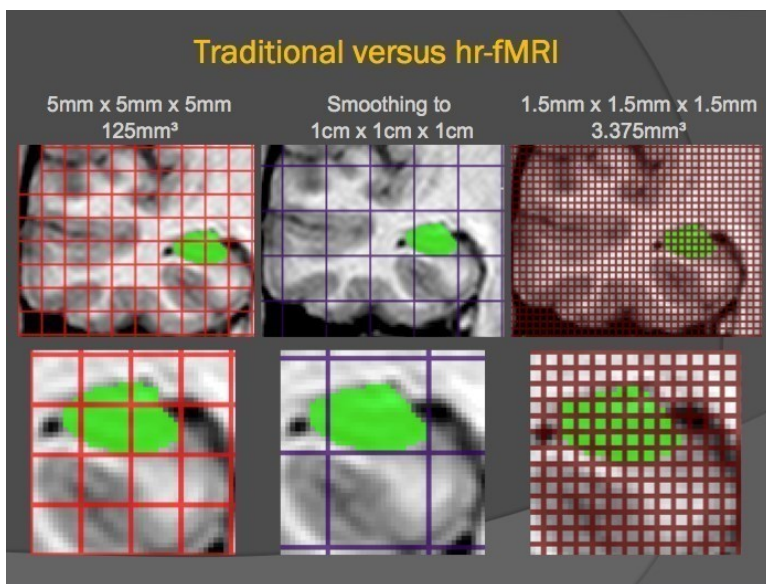


Figure 1.4: Comparison of typical and high-resolution fMRI voxel size and their application to the medial temporal lobe (MTL)
(From Malykhin N)

Information flows between subfields in a transverse manner across the hippocampus.

Two pathways of intrahippocampal information flow across hippocampal subfields are the direct (See Figure 1.5) and polysynaptic (See Figure 1.6) pathways. The polysynaptic pathway includes the perforant and temporo-ammonic pathways described in animal literature (Aksoy-Aksel &

Manaham-Vaughan, 2013). The direct pathway is associated with semantic memory, while the polysynaptic pathway is associated with episodic memory (Duvernoy, 2013). In the polysynaptic pathway information flows from the entorhinal cortex to the DG, then the CA, then the Sub and back to the entorhinal cortex. Input for this pathway originates in temporal, occipital and posterior parietal association cortices. Polysynaptic output extends to the fimbria, and the fornix, which extends to the anterior thalamic nucleus (thalamus), posterior cingulate cortex, retrosplenial cortex and anterior cingulate cortex (Duvernoy, 2013) (See Figure 1.7 from Duvernoy, 2013).

Understanding these pathways provides us with information about how the hippocampus is connected to the rest of the cortex, and may provide support for hippocampal activity observed based on what cortical regions would be assumed to be active.

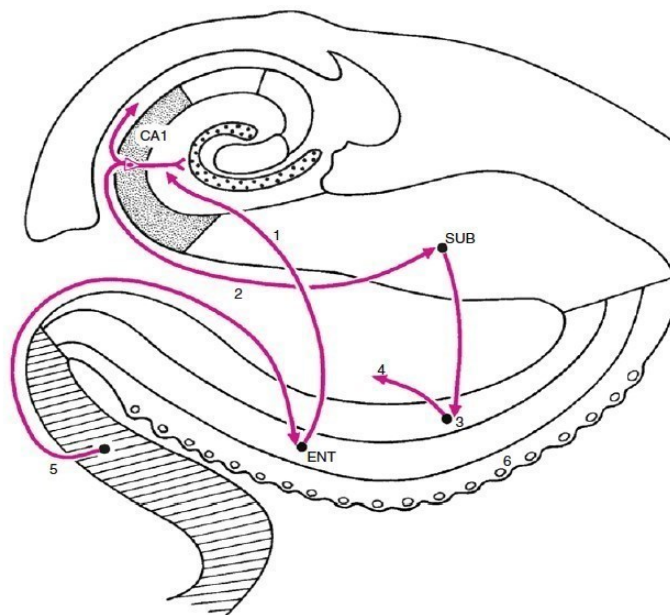


Figure 1.5: Direct intrahippocampal pathway. The entorhinal area (ENT) (layer III) projects directly onto (1) CA1 pyramidal neurons, which innervate (2) the subiculum (SUB). Subicular axons project back to the deep layers of the entorhinal cortex (3). The neurons of these layers send axons to the association cortex (4). The direct pathway receives input through perirhinal cortex (5) & layer II of the entorhinal cortex (Duvernoy, H.M., Cattin, F., Risold, P.Y. (2013). *The human hippocampus: Functional anatomy, vascularization, and serial sections with MRI*. Berlin Heidelberg: Springer-Verlag)

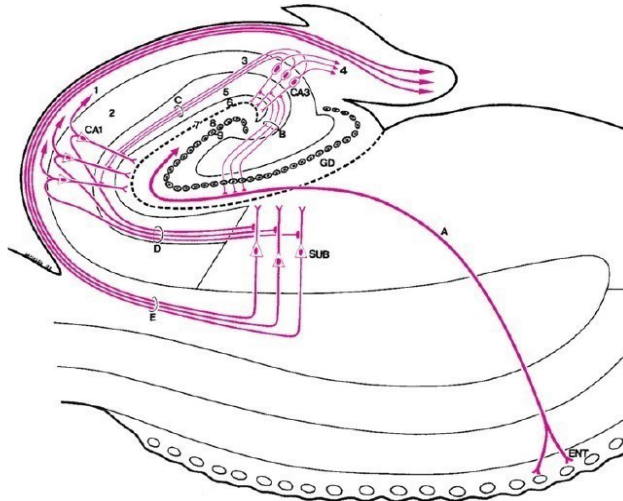


Figure 1.6: Polysynaptic intrahippocampal pathway. A-E are parts of the neural chain forming the polysynaptic intrahippocampal pathway. Cornu Ammonis: 1 alveus, 2 stratum pyramidale, 3 Schaffer collaterals, 4 axons of pyramidal neurons (mainly to septal nuclei), 5 strata lacunosum and radiatum, 6 stratum moleculare, 7 vestigial hippocampal sulcus. Gyrus dentatus (GD): 8 stratum moleculare, 9 stratum granulosum. CA1, CA3 fields of the cornu Ammonis, SUB subiculum. ENT (Layer II of the entorhinal area) is the origin of this chain; its large pyramidal neurons are grouped in clusters, giving a granular aspect at the entorhinal surface.

(Duvernoy, H.M., Cattin, F., Risold, P.Y. (2013). *The human hippocampus: Functional anatomy, vascularization, and serial sections with MRI*. Berlin Heidelberg: Springer-Verlag)

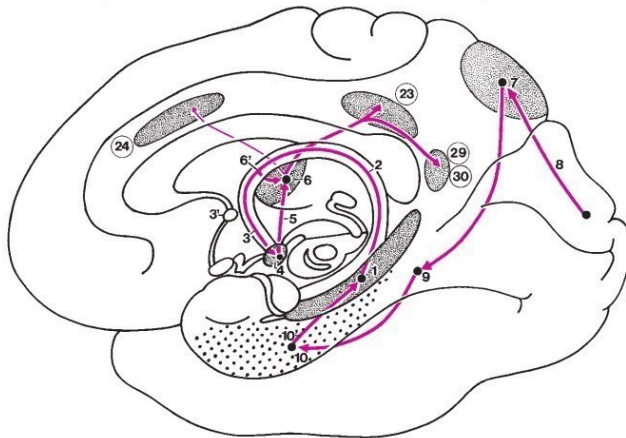


Figure 1.7: Cortical connections of the polysynaptic intrahippocampal pathway. Hippocampal outputs fibers to the cortex: arising from the hippocampus (1), fibers successively reach the body (2) and column (3) of fornix (3', anterior commissure), the mamillary body (4), and then, via the mamillothalamic tract (5), the anterior thalamic nucleus (6); some fibers reach this nucleus directly (6'); from the anterior thalamic nucleus, the main cortical projections are the posterior cingulate (area 23) and retrosplenial (areas 29, 30) cortices; some fibers may project to the anterior cingulate cortex (area 24) (see p. 33). Input fibers from the cortex to hippocampus: the posterior parietal association cortex (7) in relation to the superior visual system (8) projects via the parahippocampal gyrus (9) to the entorhinal area (10); 10', perforant fibers

(Duvernoy, H.M., Cattin, F., Risold, P.Y. (2013). *The human hippocampus: Functional anatomy, vascularization, and serial sections with MRI*. Berlin Heidelberg: Springer-Verlag)

The hippocampus can also be divided along its longitudinal axis into subregions known as the hippocampal head, body and tail (Duvernoy, 2005) or anterior and posterior sections (See

Figure 1.8 from Malykhin et al., 2007). In the animal literature these subregions are known as the ventral and dorsal hippocampus respectively (see Figure 1.9 from Strange et al., 2014). All subregions of the hippocampus contain the CA, DG and Sub subfields, but the proportion of these subfields varies along the longitudinal axis (Malykhin et al., 2010).

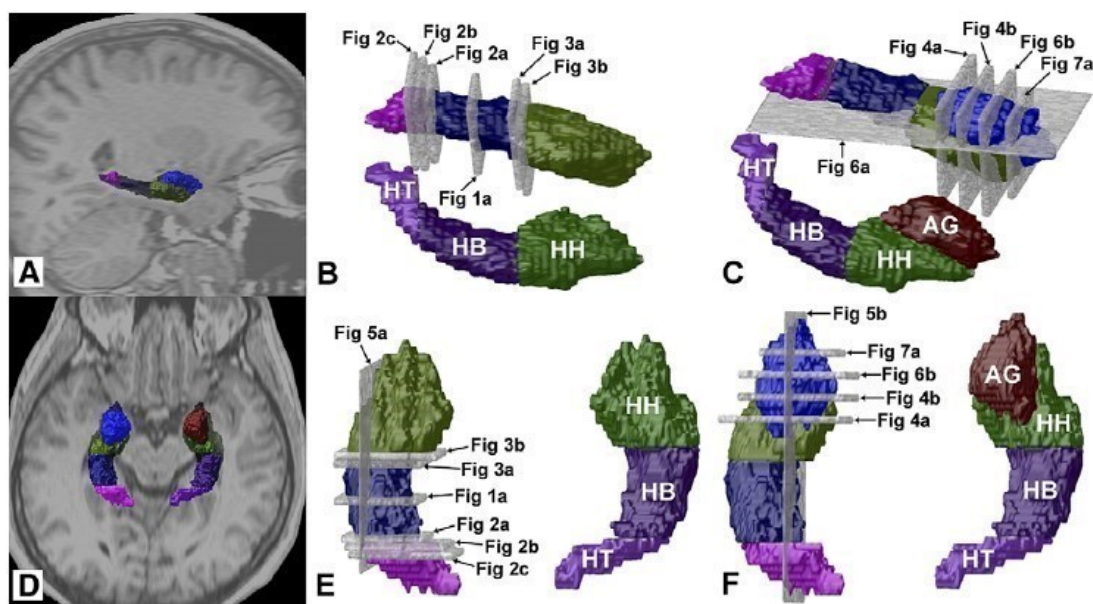


Figure 1.8: Three-dimensional renderings of the hippocampus and amygdala. A: 3-D hippocampus and amygdala (left) placed in situ in the sagittal slice corresponding to Fig. 5b. B-C: 3-D hippocampi and amygdalae viewed from the right with reference to slices from the two dimensional figures. D: 3-D hippocampi and amygdalae placed in situ in the axial slice corresponding to Fig. 6a. E-F: 3-D hippocampi and amygdalae viewed from the top with reference to slices from the two-dimensional figures.

(Malykhin, N.V., Bouchard, T.P., Ogilvie, C.J., Coupland, N.J., Seres, P., Camicioli, R., (2007). Three-dimensional volumetric analysis and reconstruction of amygdala and hippocampal head, body and tail. *Psychiatry Research: Neuroimaging*. 155(2), 155–165.)

For the purpose of this study we divided the hippocampus into head, body and tail regions based on anatomical landmarks (Duvernoy, 2005) that can be identified on high-resolution MRI images (Malykhin et al., 2007, 2010) to provide more anatomical specificity when analyzing our results. Previous literature that separates the hippocampus into anterior and posterior sections often simply divides the hippocampus in half (Poppenk et al., 2013) which means the anterior hippocampus would be equal to our hippocampal head and the anterior part of the hippocampal

body, and the posterior hippocampus would be equal to our hippocampal tail and the posterior part of the body.

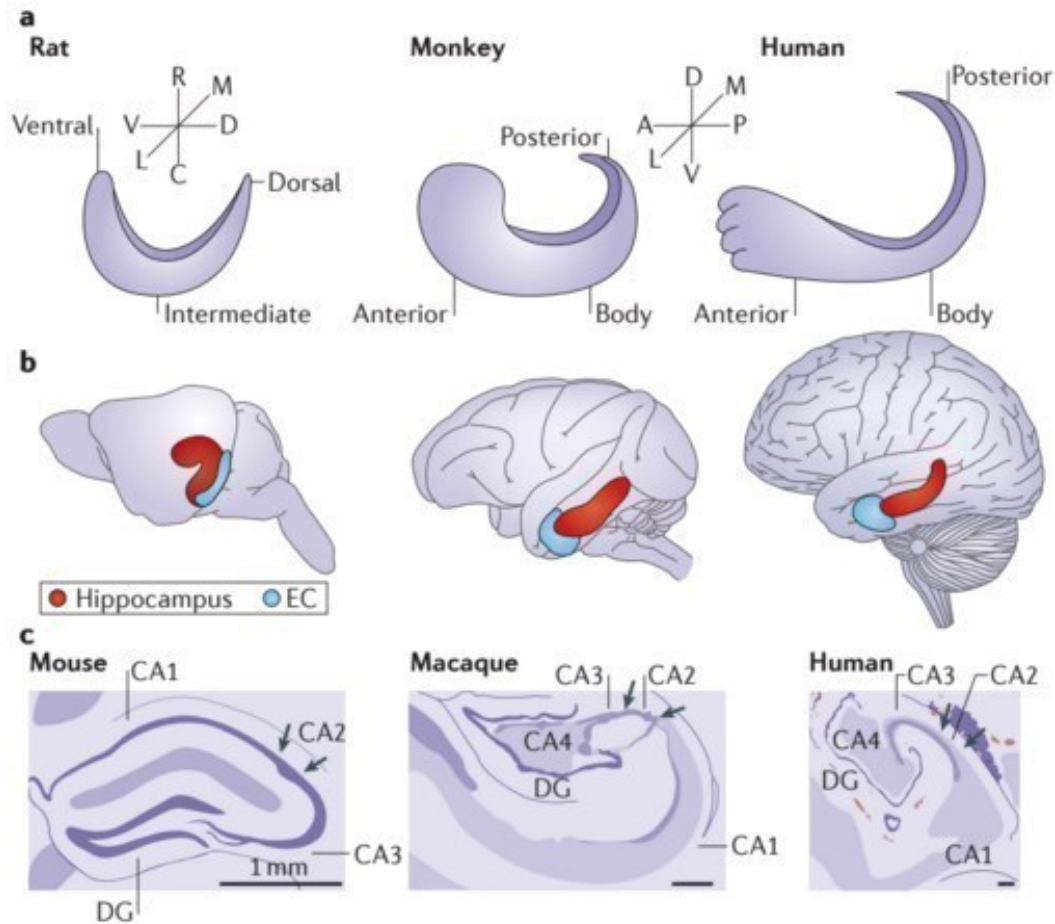


Figure 1.9: Figure 1 | **Cross-species comparison of hippocampal anatomy.** **a** | Schematic illustrations of the orientation of the hippocampal long axis in rats, macaque monkeys and humans. The longitudinal axis is described as ventrodorsal in rodents and as anteroposterior in primates (also referred to as rostrocaudal in non-human primates). There is currently no precise anatomical definition for a dorsal (or posterior) portion of the hippocampus relative to a ventral (or anterior) one, although in general, topologically, the former is positioned close to the retrosplenial cortex and the latter close to the amygdaloid complex. Note that a 90-degree rotation is required for the rat hippocampus to have the same orientation as that of primates. In primates, the anterior extreme is curved rostromedially to form the uncus. **b** | The full long axis of the hippocampus (red) can be seen in brains of rats, macaque monkeys and humans, with the entorhinal cortex (EC) shown in blue. **c** | Drawings of Nissl cross-sections of mouse, rhesus and human hippocampi. A, anterior; C, caudal; D, dorsal; DG, dentate gyrus; L, lateral; M, medial; P, posterior; R, rostral; V, ventral. Panel **a** is adapted with permission from REF. 171 (Insausti 1993), Copyright © 1993 Wiley-Liss, Inc., A Wiley Company. Panel **c** is from REF. 54 (Hawrylycz et al. 2012), Nature Publishing Group. (Strange, B.A., Witter, M.P., Lein, E.S. & Moser, E.I. (2014). Functional organization of the hippocampal longitudinal axis. *Nature Reviews Neuroscience*. 15, 655-669.)

Structural connectivity suggests hippocampal subregions may be functionally differentiated. The anterior hippocampus primarily projects to anterior cortical regions while the

posterior hippocampus primarily projects to more posterior cortical regions (See Figure 1.10 from Poppenk et al., 2013). While there is some overlap in cortical connectivity of the anterior and posterior hippocampus, the majority of their connectivity is quite different. For instance, both anterior and posterior hippocampal subregions project to the entorhinal cortex, but to different bands. They have little direct connectivity and may communicate indirectly via the perirhinal and parahippocampal cortex (Poppenk et al., 2013). Schultz et al. (2012) showed that the perirhinallateral entorhinal pathway was more involved in the retrieval of faces, while the parahippocampalmedial entorhinal pathway was more involved in the retrieval of scenes. This provided support for the theory of differential involvement of the perirhinal cortex and lateral entorhinal cortex vs the parahippocampal cortex and medial entorhinal cortex in spatial vs. nonspatial tasks, and provides further evidence for functional specialization of hippocampal subregions. Parahippocampal cortex is located primarily within the posterior hippocampus (body and tail), while entorhinal cortex and perirhinal cortex are located within the anterior hippocampus (head).

Other differences in anatomical cortical connectivity can be seen when comparing different sensory inputs of the hippocampus (See Figure 1.11). There is some overlap across subregions where auditory and somatosensory stimuli are connected to the intermediate hippocampus (hippocampal body), but overlap with anterior (head) and posterior (tail) sections as well. Olfactory and gustatory stimuli have dominant connections to the anterior hippocampus, while visual and vestibular/proprioception stimuli have dominant connections to the posterior hippocampus (Small et al., 2002). Although it might not be directly linked to the task used in the present study, the differential functional connectivity of the hippocampus for various sensory inputs is further support for functional specialization of hippocampal subregions.

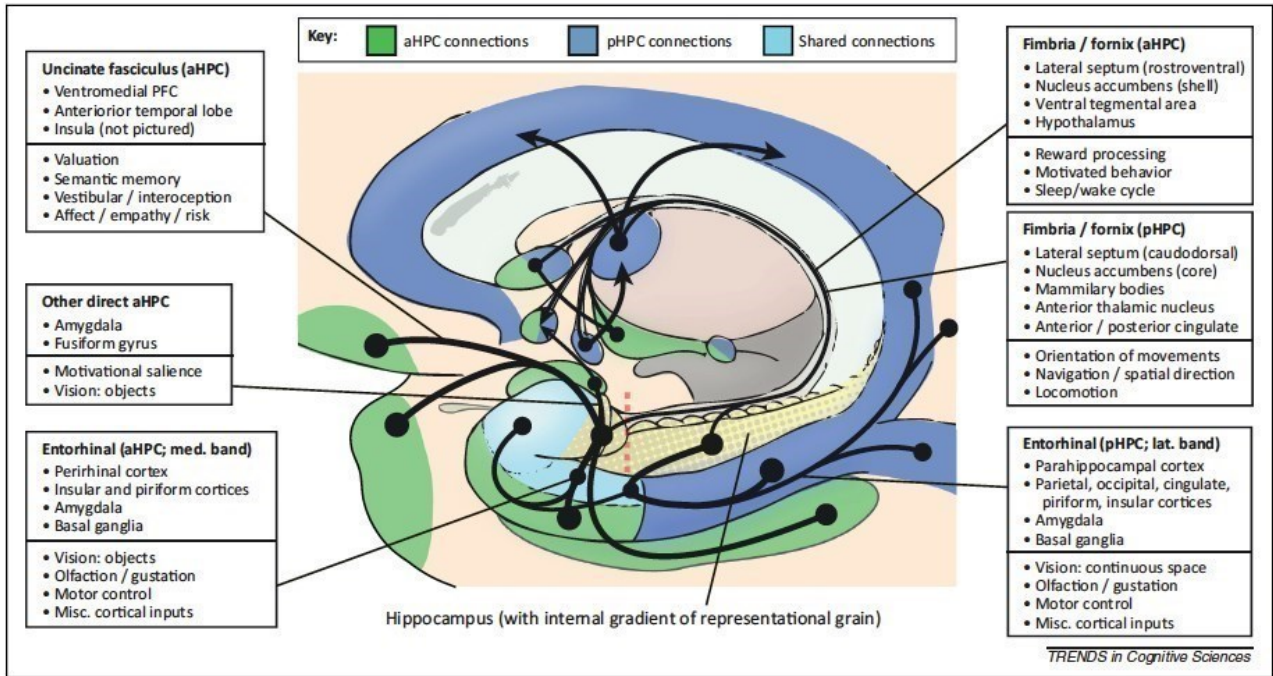


Figure 1.10: Model of long-axis hippocampal specialization. Hippocampal connections (thick black lines) are depicted with reciprocal termination points (black dots). The aHPC and pHPC are separated by the plane that contains the uncus apex (dashed red line). The information hypothetically carried on each pathway is shown in boxes. (Poppenk, J., Evensmoen, H.R., Moskovitch, M. & Nadel, L. (2013). Long-axis specialization of the human hippocampus. *Trends in Cognitive Neuroscience*. 17(5), 230-240.)

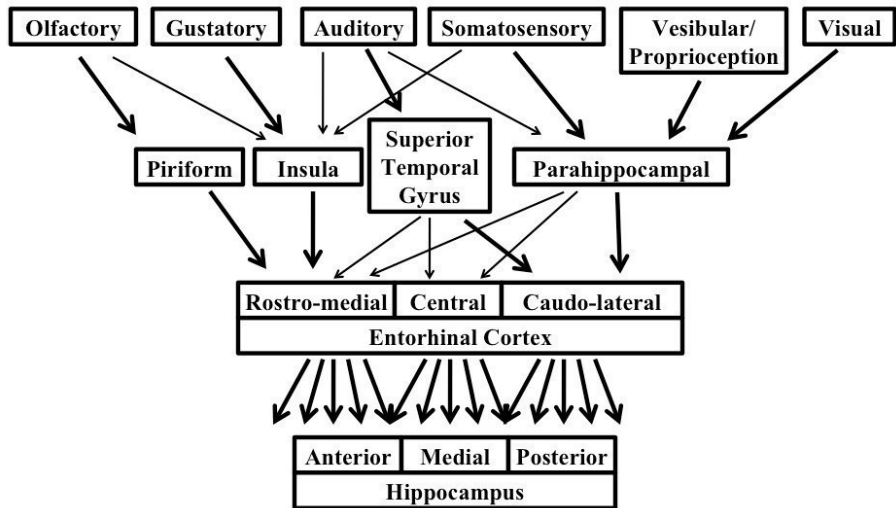


Figure 1.11: Sensory input onto the long-axis of the hippocampus. Based on a figure by Small, (2002).

The majority of fMRI studies on the human hippocampus divide it into anterior and posterior sections, potentially missing important information about the intermediate hippocampus.

For instance, Small et al. (2002) studied hippocampal activity across the hippocampal head, body

and tail during a memory task using fMRI. Participants studied stimuli across three phases: visual faces, auditory names, and visual faces paired with auditory names. A posterior-anterior activation gradient with the largest activation found in the posterior hippocampus was observed during the faces-only condition, while an anterior-posterior gradient with the largest activation found in the anterior hippocampus was observed during the names only condition. The authors argued that if the hippocampus did not engage in combining the face-name pairs the activity observed during the face-name condition would simply be a summation of the activity observed in the face-only and name-only conditions. However, the summation of activity was not observed, and the intermediate hippocampus showed the greatest activation during the face-name pairs condition. The authors suggest this pattern of activity is indicative of the hippocampus forming associations between separate stimuli. While anatomical connectivity would suggest the anterior hippocampus should be engaged while hearing names and the posterior hippocampus should be engaged while viewing faces, it appears as though the activity is not restricted to only these areas.

The current study aimed to separate the hippocampus into its anatomical subregions of the head, body and tail (Duvernoy, 2005) to provide a more accurate picture of activity along the entire long axis of the hippocampus. Furthermore, this approach allows us to address the possibility of a gradient in activity (head, body and tail) as opposed to a dichotomy (anterior/posterior).

1.3: Hippocampal Subfields and Subregions in Memory Function

The current study aimed to address the important gap in the literature of how hippocampal subregions and subfields are involved in the encoding of new episodic memories. Using highresolution fMRI we assessed activity across subregions and subfields during an episodic memory

task.

While disagreements do exist, there is evidence suggesting activity in the CA1 area demonstrates a match/mismatch/novelty signal (Duncan et al., 2012), while activity in the DG/CA3 changes with repetition, degree of change in stimuli and behavioural performance (Reagh et al., 2014, Stokes et al., 2015). The match/mismatch/novelty signal observed in CA1 by Duncan et al. (2012) is characterized by a linear change in activity that correlated with the degree of change in a scene. Reagh et al. (2014) found that activity in the DG/CA3 subfield was reduced with repetition of stimuli, where greater activity suppression was related to better behavioural performance.

Using structural MRI, a previous study from our lab (Travis et al. 2014) found that performance on the Wechsler Memory Scale (WMS---IV; Pearson Education I., 2009) was associated with specific hippocampal subfield and subregion volumes. (For a more thorough description of the Wechsler Memory Scale see Section 2.3: Memory Task) DG volume in the hippocampal body was associated with visual-spatial memory, while CA1-3 volume was associated with both visual-spatial memory and visual-content memory. The strongest correlations were observed for scores in the Designs subtest. Therefore our fMRI task was designed to mimic this task and produce the strongest activation in the hippocampus and its subfields. A single previous adaptation of the WMS for use in an fMRI paradigm was completed by Neuner et al.

(2007). The study used an adaptation of the Paired Associates subtest and found no significant activation in the hippocampus, but did find activation in other cortical regions. In contrast the task used in our study is designed to study visual memory, while the Paired Associates subtest is designed to test auditory memory. In the current study we employed an episodic memory task based on the Wechsler Memory Scale (WMS---IV; Pearson Education I., 2009) Designs Subtest, which tested visual memory. Such translational design allows us to determine whether or not our

previous volumetric findings are indicative of functional activation differences between hippocampal subfields.

It is well accepted the hippocampus plays a role in spatial memory, which may be due to the associative nature of encoding spatial locations (Piekema et al., 2010). Although there is no clear agreement in the field, some evidence suggests the posterior hippocampus is more active than the anterior hippocampus for spatial memory tasks (Strange et al., 2014). The current study aimed to address subregion and subfield involvement in spatial memory by measuring activity during the encoding of our spatial task.

A meta analysis of studies on hippocampal subregions suggests the anterior and posterior regions play different roles in memory. Some studies have reported that for episodic memory the anterior hippocampus is active during encoding (Spaniol et al., 2009; De-Vanssay-Maigne et al., 2012) and the posterior hippocampus is active during retrieval. However there is contradictory research suggesting the entire hippocampus along the long axis is engaged for encoding, or that encoding effects observed may be due to novelty effects (Poppenk et al., 2013). Other studies have reported anterior hippocampal activity to be associated with memory for global spatial representations and general features of a memory with posterior hippocampal activity associated with local spatial representations and more detailed features of a memory (Poppenk et al., 2013). The current study aimed to further contribute to our knowledge of this subregional specificity by indicating whether or not all anatomical subregions are simultaneously involved in the encoding of episodic memories and if they are equally involved during the encoding of spatial and content information.

1.4: Models of Hippocampal Function

The goal of the current study was to investigate how the hippocampus encodes new episodic memories. Different theories suggest the hippocampus works as a single unit, in discrete sections or in interconnected sections with preferred roles (See Figure 1.12). Understanding which model best describes hippocampal activity can provide us with information that either supports or rejects hippocampal functional specialization. We investigated hippocampal function by assessing subregion and subfield activity. If a function was specific to a particular subregion and that subregion was damaged, we would expect for that function to be severely impaired and the person or animal to be unable to complete that function. However, if subregions are all functionally involved then it is less likely that damage to a particular area would result in complete loss of that function. Performance may be impaired, but the function should not be wiped out entirely.

The first model of hippocampal function suggests the hippocampus functions as separate independent units. This is based on studies by Anderson et al. (1971) and Bliss and Lomo (1973) that demonstrated activation that spread transversely across the hippocampus and that long term potentiation (LTP) occurs during this spread of activation. This theory suggests the hippocampus is made up of separate sections with independent circuits across its length (Small et al., 2002).

The second model of hippocampal function suggests the hippocampus acts as a single functional unit. Studies by Amaral and Witter (1989) and Pare et al. (1994) that showed anterograde and retrograde tracers and electrical activity travelled the length of the hippocampus provide support for this theory of hippocampal function. According to this theory, the hippocampus should function as a single unit regardless of cortical input (Small et al., 2002).

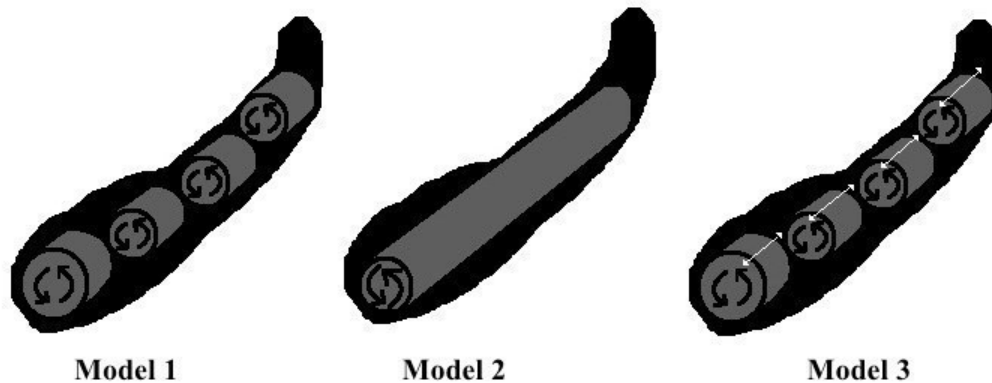


Figure 1.12: Three models describing the functional organization of the hippocampus. Based on a figure from Small, (2002)

The third model of hippocampal function suggests the hippocampus is made up of subregions that are interconnected but functionally segregated. Small et al. (2002) observed a gradient in fMRI activation where the anterior hippocampus was most active when participants heard names and the posterior hippocampus was most active when they viewed faces. Retrieval of face-name pairs elicited activity in the intermediate hippocampus. Retrieval activity was observed in a different region for combined faces and names than for encoding of faces or names individually. This is indicative of functionally separate, yet connected subregions. The current study assesses hippocampal subregion circuitry by measuring hippocampal activation across its anatomical subregions during an episodic memory task.

1.5: Objective

Interest in the long axis of the hippocampal formation as well as in function of its subfields has been increasing since the introduction of high-resolution structural and functional MRI has allowed separation of the hippocampus into its anatomical parts. Recent human fMRI studies indicate that, much like the more popular transverse axis, the long axis of the hippocampus needs to be viewed as a functional circuit. As has been shown with previous structural MRI studies from our lab, circuit analysis of the long axis provides unique insight into the role played by the hippocampal subfields and subregions in episodic memory.

The main goal of the present study was to investigate how the hippocampus as a whole, and its smaller subsections (subfields and subregions) are involved in the encoding of new episodic memories using high-resolution functional Magnetic Resonance Imaging (fMRI). The second goal was to investigate the role of these subfields and subregions in the encoding of different types of episodic memory, in particular content, spatial, and associative memory. Based on a previous study in our lab (Travis et al., 2014) we hypothesize subfields and subregions will be differentially active during the encoding of different conditions of our task. Specifically, we anticipate the posterior hippocampus to be more active during the spatial task than the anterior hippocampus, and the DG to be more active than the CA1-3 and Sub across tasks.

Understanding the similarities and differences in activity across subfields and subregions will contribute to current knowledge of how the hippocampus works. Our study aimed to determine whether the hippocampus acts as a single unit or multiple units that are either connected or independent.

Chapter 2: Material and Methods

2.1: Participants

A total of 29 healthy volunteers were recruited to participate in the current study. All participants were screened to ensure they had no personal history of psychiatric or neurological illness as assessed by a structured interview (Anxiety Disorders Interview Schedule-IV: Brown et al., 2001) and were excluded if they were on medication that could affect cognition such as antipsychotics, benzodiazepines, antidepressants, anti-cholinergic medications or alcohol. Medical exclusion criteria were defined as active and inactive medical conditions that may interfere with normal cognitive function: cerebrovascular pathology, tumors or congenital malformations of the nervous system, diabetes, multiple sclerosis, Parkinson's disease, epilepsy, dementia, organic psychosis (other than dementia), schizophrenia, and stroke. Four participants were excluded from analyses due to excessive head motion (>25% of volumes had to be removed) or deciding not to continue with the study. A final sample of 25 participants (13 female, 20-33 years old) with a mean age of 25.44 years (SD: 3.03) was used for analysis. Our participants were all right-handed.

Written, informed consent was obtained from each participant. The study was approved by the University of Alberta Health Research Ethics Board.

2.2: Stimuli

Participants studied rectangular 4x4 grids with 4 abstract symbols spaced throughout the boxes (See Figure 2.1). The abstract symbols used for the study were obtained from the Wechsler Memory Scale (Wechsler, 2009) Design and Symbol Span subtests. We scanned pages from a paperback version of the task, cropped all images into the same dimensions and changed them into identical pixel quality. The task was modelled after the Designs subtest, but Symbol Span images

were used to increase the number of stimuli so participants could complete more trials. The presentation of stimuli was randomized for each participant, so each person saw abstract images in a different temporal order and spatial configuration.

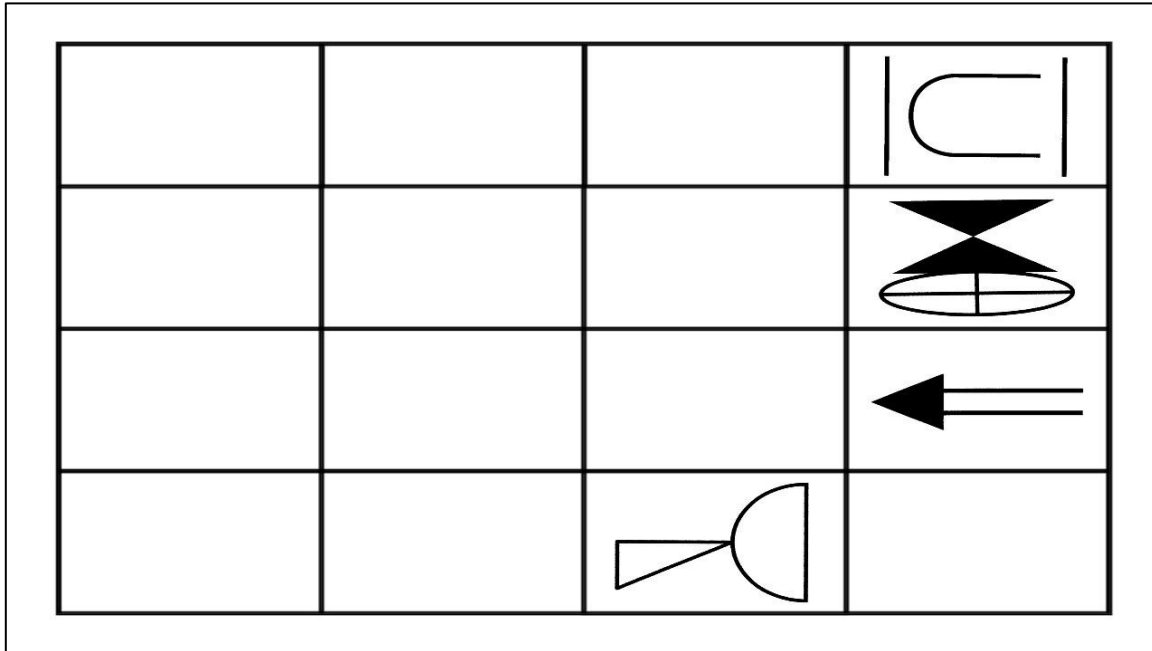


Figure 2.1: One example of a 4x4 grid containing 4 abstract symbols that participants would view during the encoding phase of all conditions of the task

2.3: Memory Task

Participants were told they were performing 2 tasks: a memory task and a number judgment task. The memory task used in the current study was based on the Designs subtests of the Wechsler Memory Scale (WMS-IV; Pearson Education I., 2009). The Wechsler Memory Scale is a paperbased clinical memory test that assesses different forms of memory. The Designs subtest in particular assesses both visual-spatial and visual-content memory. The examiner shows the examinee a grid containing 4-8 abstract symbols on a page for 10 seconds. Immediate memory is assessed just after the grid is removed, and delayed memory is assessed after a longer period of

time has passed and other tests have been completed. Memory performance is tested in two different ways: the examinee recreates the grid by choosing the abstract symbols they remember and placing them in the corresponding locations, and by indicating which grid out of a group of grids corresponds to what they previously studied. Scores are broken down into visual-spatial and visual-content memory. Visual-spatial memory scores are given for correct placement of images on the grid. Visual-content memory scores are given for choosing the correct abstract images (Maccow, 2011). For the current study's memory task, participants were shown 4 abstract symbols placed randomly in a 4x4 grid. They were cued to focus on different aspects of the grid by a letter (S, L or B) that appeared in the middle of the screen prior to the grid. Letters represented the 3 different conditions: Symbol, Location and Both. For the Symbol condition participants were instructed to remember what symbols appeared regardless of their location (See Figure 2.2 for visual explanation). For the Location condition participants were instructed to remember where the symbols appeared in the grid regardless of what the symbols were (See Figure 2.3 for visual explanation). For the Both condition participants were instructed to remember both what symbols they saw and where they appeared in the grid (See Figures 2.4 and 2.5 for visual explanation). Participants viewed the grid for 10 seconds. Everyone was read pre-written instructions to ensure they all received the same information.

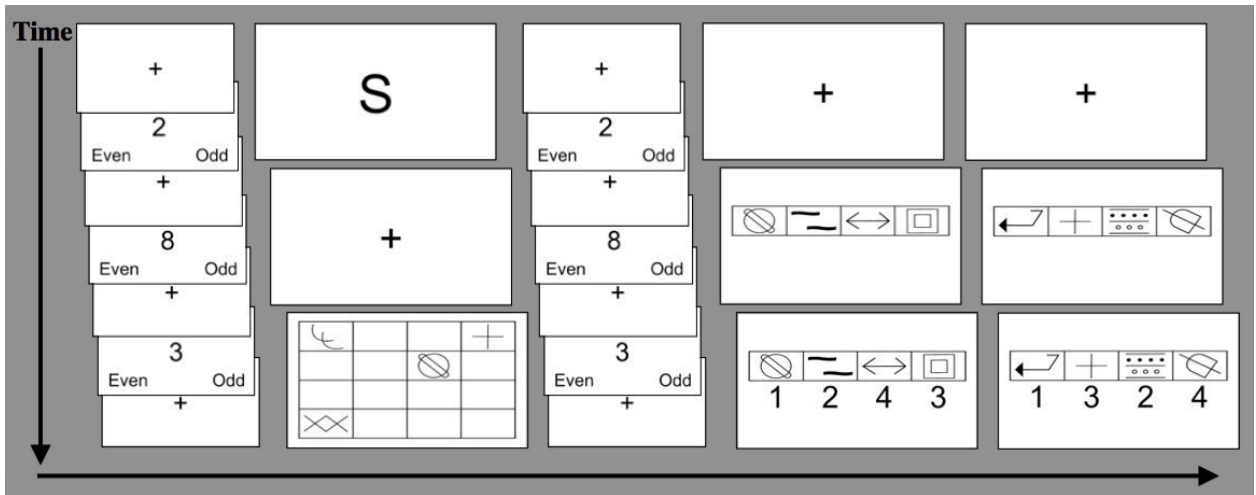


Figure 2.2: Visual depiction of the symbol condition of the memory task

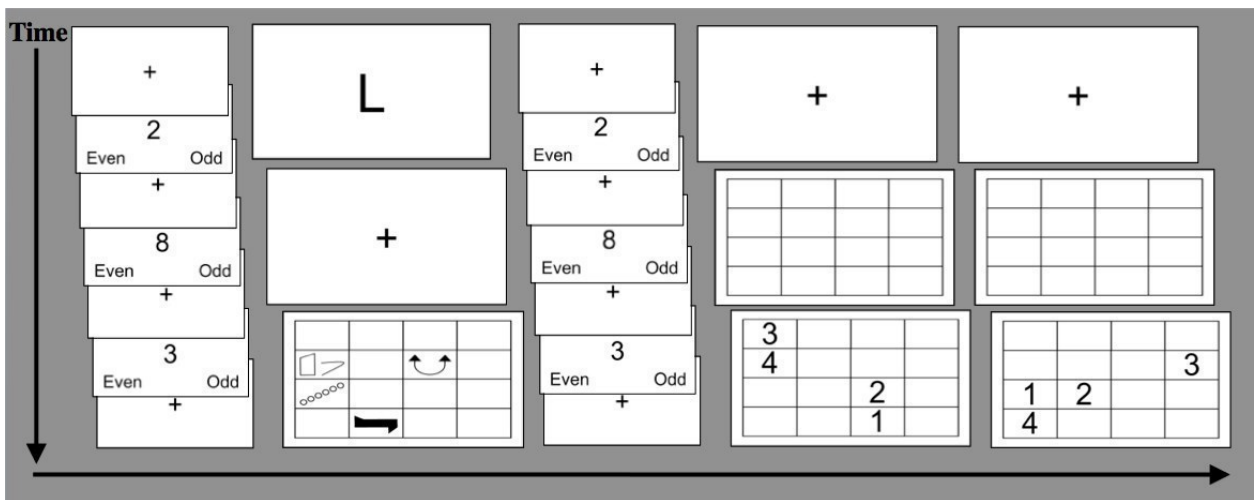


Figure 2.3: Visual depiction of the location condition of the memory task

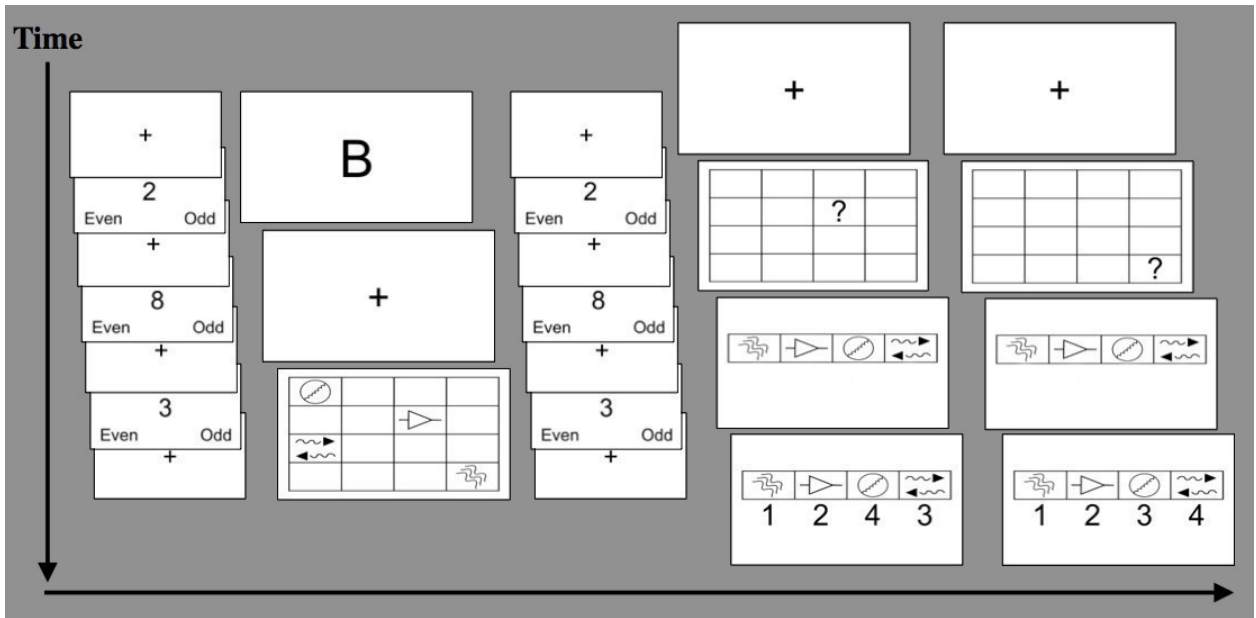


Figure 2.4: Visual depiction of the both condition of the memory task with location cues.

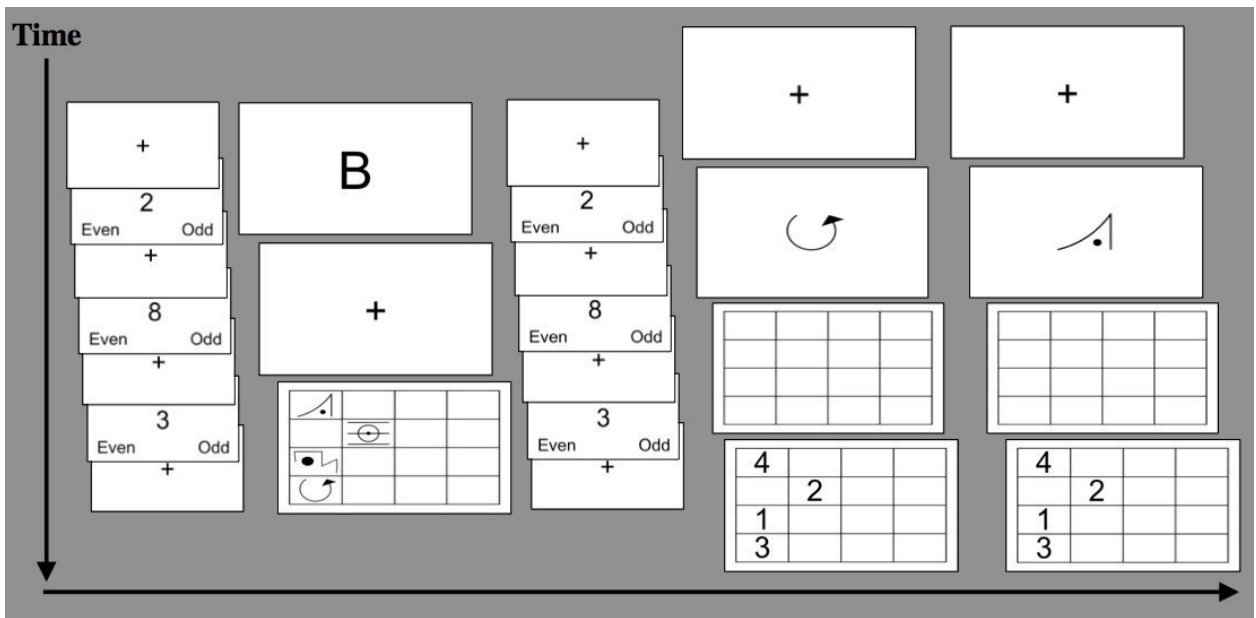


Figure 2.5: Visual depiction of the both condition of the memory task with symbol cues.

For the retrieval phase of the task, participants were asked to indicate by button press which symbol they previously viewed (Symbol/Both) or which location previously contained a symbol (Location/Both). They completed 2 retrievals for each encoding trial. During retrieval of the Symbol condition participants viewed 4 symbols for 5 seconds. After the first 2 seconds the numbers 1 to 4 appeared under the symbols in a randomized order and they had 3 seconds to respond. During retrieval of the Location condition participants viewed a blank 4x4 grid for 2 seconds. After 2 seconds the numbers 1 to 4 appeared randomly in the boxes for 3 seconds. The Both condition retrieval was sectioned into 2 parts – participants were either presented with a symbol they previously viewed and asked to indicate where in the grid it appeared, or they were given a location and asked which symbol appeared in that location. Participants were given a cue (a location or a symbol) for 2 seconds, then presented with either 4 symbols or a blank grid for 2 seconds, and randomized numbers for 3 seconds. Each run of the task included all 3 conditions (Symbol, Location and Both) in a randomized order.

Inter-mixed with the memory task was our baseline task: number judgment (odd/even). Participants were presented with a single number in the middle of the screen and asked to indicate whether the number was odd or even. The odd and even cues were visible in the bottom left and right corners of the screen. Participants were randomly assigned arrangement of odd and even cues. (Approximately half of the participants completed the task with “odd” in the bottom left corner, while the other half completed the task with “odd” in the bottom right corner.) Numbers appeared on the screen for 1.25 seconds. At this speed, participants were actively engaged in the task. Participants were instructed to focus on the task at hand and to actively engage in the number judgment task to ensure they were not rehearsing the memory task.

2.4: Experimental Design

Participants were given instructions and completed a practice session (without responding) prior to entering the scanner to ensure they understood the task. Once participants were set up inside the scanner they had the opportunity to adjust their screen, and become familiarized with the button presses.

Next, participants had the opportunity to complete a practice session of the memory task while inside the scanner before collection of fMRI data. Correct answers turned blue after a delay so participants could see if they had responded correctly.

After all of the setup and practice sessions were complete, participants completed 12 runs of the task inside the scanner. Each run of the task contained one trial of each condition (Symbol, Location and Both) and lasted approximately 2.5 minutes with a 3 minute break in between. The 12 runs of the task were randomized for each participant ensuring that participants completed the Symbol, Location and Both conditions in a random and different order each time.

2.5: Data Acquisition

High-resolution anatomical images, full-brain anatomical images, high-resolution functional images and field maps were acquired using the 4.7 Tesla Varian MR Imaging System at the Peter Allen MR Research Centre. The images were acquired in 2 scanning sessions: in the first session we acquired Coronal FSE and MPRAGE images, and in the second session we acquired Axial FSE and EPI (functional) images.

High-resolution structural images were acquired using a 2D T2-Weighted Fast Spin Echo (FSE) Sequence aligned along the anterior-posterior commissure (AC-PC) line. The Coronal FSE [TR: 11000 ms, TE: 39 ms, FOV: 200 x 200 mm², Voxel Size: 0.52 x 0.68 x 1 mm³, Echo Train Length: 4, 90 Slices] was used for tracing hippocampal subfields and subregions, while the Axial FSE [TR: 7000 ms, TE: 39 ms, FOV: 210 x 200 mm², Voxel Size: 0.52 x 0.68 x 1mm³, 55 Slices] was used to help improve accuracy when registering volumes as functional volumes were acquired axially (See Figure 2.6).

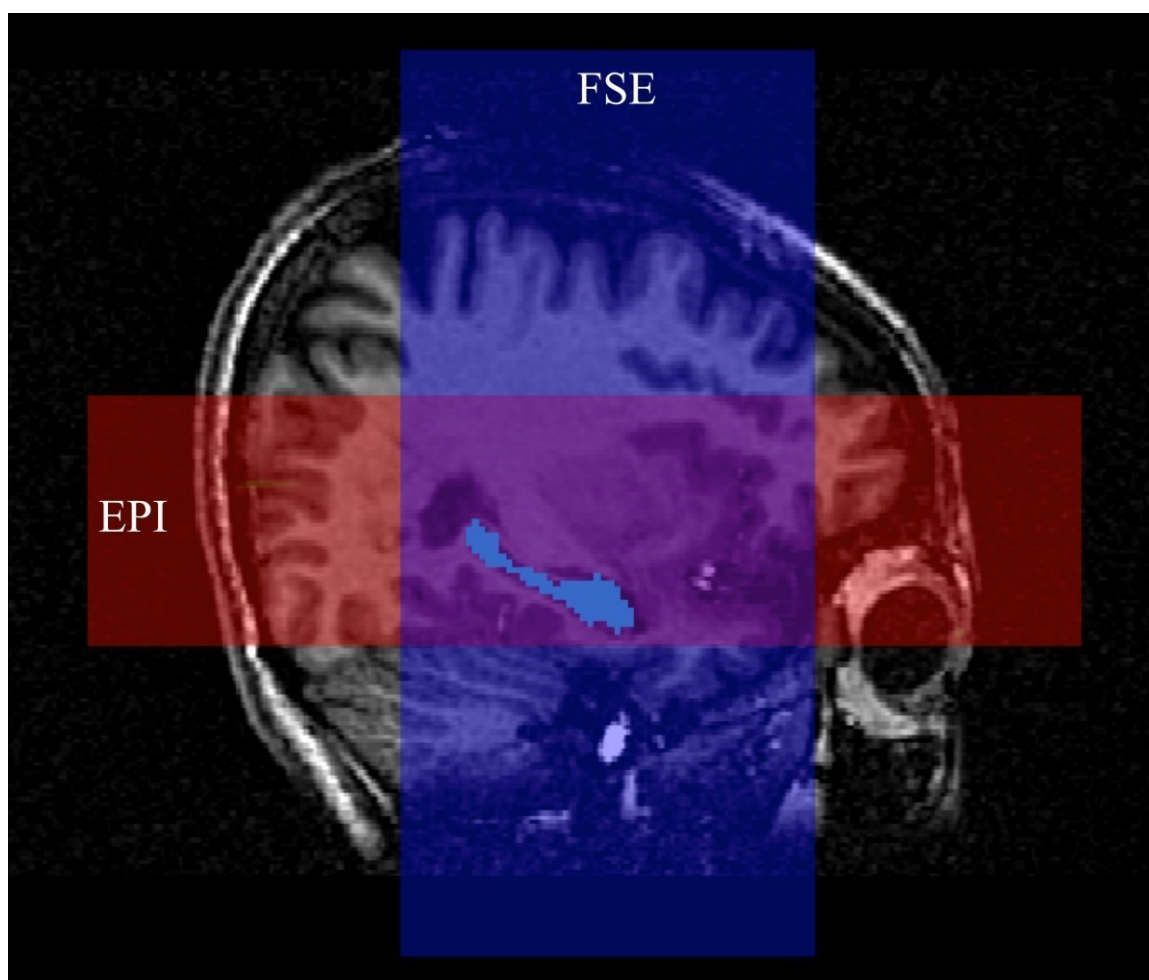


Figure 2.6: Brain coverage of high-resolution images. A single participant's full-brain t1-weighted MPRAGE is shown in the background. The anatomical high-resolution image (FSE) used to trace ROIs is shown in blue. The functional high-resolution (EPI) image is shown in red. Segmented hippocampal ROI is shown in light blue.

Full-brain anatomical images were acquired using a T1-Weighted 3D Magnetization Prepared Rapid Gradient-Echo (MPRAGE) sequence [TR: 8.5 ms, TE: 4.5 ms, Inversion Time: 300 ms, FOV: 256 x 200 x 180 mm³, Voxel Size: 1 x 1 x 1 mm³, Flip Angle: 10 degrees] and were used for tissue segmentation to create nuisance regressors during analysis.

Functional volumes were acquired axially using a T2* Sensitive Gradient Echo Planar Imaging (EPI) Pulse Sequence [TR: 2500 ms, TE: 19 ms, FOV: 168 x 210 mm², Voxel Size: 1.5 x 1.5 x 1.4 mm³ with a .1mm interslice gap, Flip Angle: 75 degrees]. During each run (of the 12 runs) of the memory task 62 EPI volumes were acquired, giving us 744 EPI volumes for each participant. Fieldmaps were acquired using a multi-echo 3D gradient echo sequence [TR: 577.8, TE: 3.56, 6.71, FOV: 192 x 168mm, Resolution: 1.5 x 1.5 mm, Slice Thickness: 1.5 mm, 35 Slices].

2.6: Hippocampal Segmentation

All manual hippocampal segmentation was completed using Freesurfer's Freeview Visualization GUI (<http://surfer.nmr.mgh.harvard.edu/>) software on T2-weighted coronal FSE images. Tracing protocols were developed with guidance from Duvernoy's (2005) anatomical atlas of the human hippocampus. Manual segmentation of hippocampal subregions (head body & tail) and subfields (CA, DG & SUB) were completed by a skilled observer (Yushan Huang) using a volumetric protocol developed by Malykhin et al. (2007) and Malykhin et al. (2010). Intra-rater and inter-rater reliability of subfields and subregions has been published in previous work from our lab (Malykhin et al., 2007, 2010). In these studies, intra-rater reliability was assessed by retracing the hippocampi of 5 subjects (10 hippocampi overall) one week after the initial tracing using intraclass correlations (ICCs) for a one-way fixed-effects design. Inter-rater (intra-rater) intraclass correlations published for this segmentation method was 0.96(0.86) for the total hippocampus,

0.95(0.92) for the hippocampal head, 0.83(0.93) for the hippocampal body and 0.95(0.88) for the hippocampal tail (Malykhin et al., 2007), 0.956 for CA1-3, 0.959 for DG and 0.972 for Sub (Malykhin et al., 2010). Subfields were first traced on anatomical coregistered T2 images, then resliced into fMRI space and manually corrected if needed (See Figure 2.7).

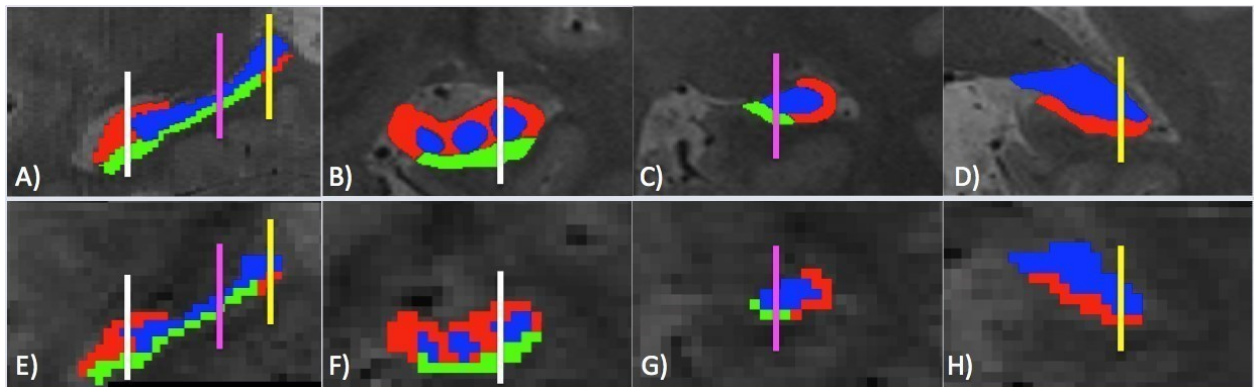


Figure 2.7: Sagittal views of the length of the hippocampus in anatomical & fMRI space. B&F) Coronal views of the hippocampal head C&G) Coronal views of the hippocampal body D&H) Coronal views of the hippocampal tail. [CA13 shown in red, DG shown in blue & Sub shown in green]

The hippocampus was divided into 3 main subfields based on our best approximation of CA1-3, DG and Sub. Our Sub volumes did not include the presubiculum and parasubiculum sections. Due to constraints of MRI imaging, the CA4 and DG regions are unable to be differentiated and CA4 is included as part of the DG.

2.7: Image Preprocessing

Structural images were acquired for various purposes and therefore provided differential coverage of the brain. To aid in registration of these volumes, images were cropped over the same brain regions across scans using Matlab (The MathWorks Inc., Natick, MA). Next, cropped images were registered using automated rigid-body transformations. The axial FSE images remained stationary while coronal FSE and MPRAGE volumes were moved to match the axial image.

Tracing of hippocampal ROIs was completed on Coronal FSE images after registration.

However, MPRAGE images were corrected for intensity non-uniformity using N3 (Nonparametric Non-uniform intensity Normalization) (McGill University, Montreal, QC) before registration. This controls for MRI signal intensity fluctuations in structural images, which helps improve the accuracy of tissue classification in later analysis. Without N3 correction, signal variation would be too large and accurate tissue segmentation analysis would not be possible on the MPRAGE images.

Using hippocampal subfield and subregion ROIs and neglecting the rest of the brain preserves statistical power and allows us to detect subtle hippocampal activation (Small et al., 2002). ROI analysis allows us to assess how the hippocampus is engaged in our task.

Functional volumes were registered manually using Freesurfer's Freeview Visualization GUI (<http://surfer.nmr.mgh.harvard.edu/>) and SPM12 (Wellcome Trust Centre for Neuroimaging, UCL, UK). The first functional volume was registered to the axial FSE image. Next, the average functional file for each participant was manually moved to align with the hippocampal masks. Once this image was manually adjusted, all functional files for that participant were then moved to match the adjusted volume. 23 out of 25 participants' functional volumes underwent fieldmap correction using SPM to help correct for distortions in the data (i.e. stretching of anterior temporal lobe and dropout). ART (Artifact Detection Tool) was used to identify volumes with head movement artifacts. If the head-movement was larger than 3 standard deviations (SDs) above the global signal mean and greater than 0.5mm per TR that individual volume was removed.

White matter (WM) and cerebrospinal fluid (CSF) masks were created by segmenting the MPRAGE volume in SPM12. These masks were then resampled into fMRI space, thresholded at 0.9 tissue probability and manually adjusted in Freeview. (Voxels that overlapped with hippocampal masks or that clearly represented other tissue types were removed.) The first 3

principle eigenvariates from raw WM and CSF signals were extracted using REX toolbox (<http://www.nitrc.org/projects/rex/>). These timecourses were filtered to co-vary out the effect of motion and then used as nuisance regressors in the general linear model (GLM) analysis.

To account for physiological noise in the fMRI data we collected heart rate and breathing information while participants were in the scanner. Using custom written code based on work by Glover et al. (2000), Birn et al. (2006), Birn et al. (2008) and Chang et al. (2009), we implemented a system that created nuisance regressor timecourses modeled after heart rate and breathing parameters. These timecourses were used in the GLM to control for fMRI signal associated with heart rate and breathing.

2.8: General Linear Model and HRF Fitting

The typical canonical BOLD (blood oxygen level dependent) response is based on visual cortex and may not be an appropriate fit for subcortical regions. Therefore this model may not effectively identify activity occurring in the hippocampus (Devonshire et al., 2012; Handwerker et al., 2004; Hrybouski et al., 2016; Pernet 2014). To assess the HRF (hemodynamic response function) in the hippocampus during encoding we deconvolved it using a Finite Impulse Response (FIR) model in Marsbar (v. 0.43; <http://marsbar.sourceforge.net>). We modeled all events with their own regression parameters (encoding of Symbol, Location and Both) for each run of the task (3 betas). After estimates of BOLD were created for each event separately, we averaged signal change across events where participants remembered at least 1 of 2 retrieval stimuli. For the Symbol condition 0.20 out of 12 trials were removed per participant on average (5 trials removed overall, SD = 0.50, Maximum number removed: 2). For the Location condition 1.32 out of 12 trials were removed per participant on average (33 trials removed overall, SD = 1.31,

Maximum number removed: 4) For the Both condition 1.20 out of 12 trials were removed per participant on average (30 trials removed overall, SD = 1.08, Maximum number removed: 3). Next, these fitted HRF timecourses were averaged across all participants (left and right hemispheres combined). This provided us with a plot of the hippocampal BOLD response with one point occurring for each TR (2.5s). Upon visual inspection of the model, it appeared as though the canonical HRF was a satisfactory fit (See Figure 2.8). The canonical HRF makes assumptions about when the peak of activity occurs, and how long it lasts (Calhoun et al., 2004). Since stimuli were presented to participants for 10 seconds we also modeled the HRF using time and dispersion derivatives in addition to the canonical double gamma function to provide more flexibility in what would be considered activity (See Figure 2.9).

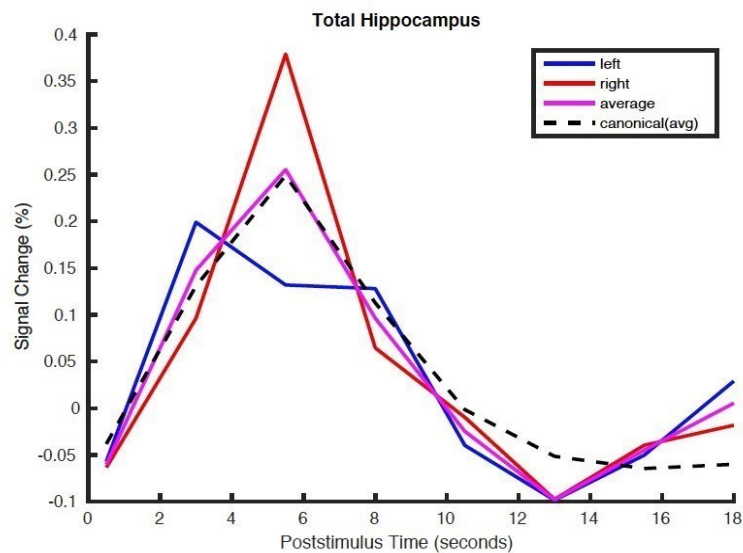


Figure 2.8: Total Hippocampal HRF fitted to Canonical Modelling. (From Hrybouksi, S)

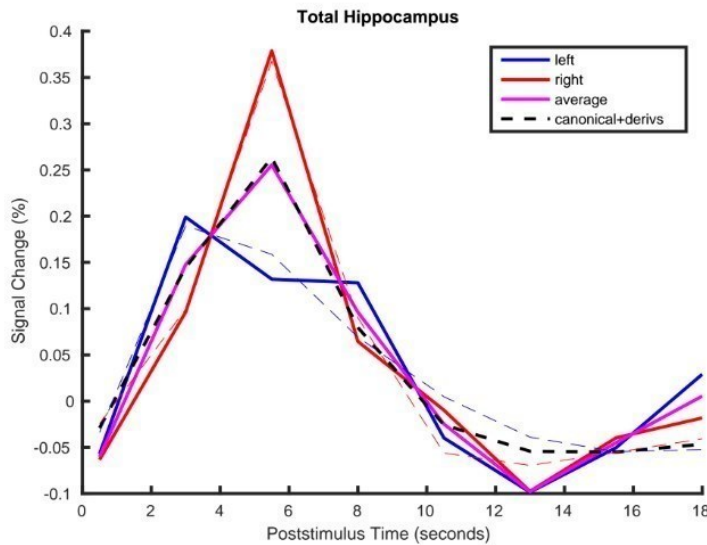


Figure 2.9: Total Hippocampal HRF fitted to Canonical + Derivative Modelling. (From Hrybouski, S)

To implement the time and dispersion derivatives we fit a double-gamma function to the mean fitted timecourse using the SIMPLEX algorithm (Nelder and Mead, 1965). This was done by using bootstrapping to optimize parameters of the HRF over 15,000 iterations, minimizing the difference between the double-gamma function and the FIR timecourse. We used the optimized double-gamma function and its first order derivative to estimate our BOLD response.

2.9: Imaging Analysis

We completed two sets of analyses using classical canonical HRF modelling and canonical with time and dispersion derivatives HRF modelling. For the classical canonical HRF modelling we completed paired t-tests, one-sample t-tests and repeated measures ANOVAs. For the canonical with time and dispersion derivatives, we used the Bootstrap technique to estimate the standard error to estimate t statistics and p values. We will discuss similarities and differences observed using different analyses.

Canonical Analysis

HRF modelling was completed using the classical canonical double-gamma function. This model is often used in fMRI research and makes assumptions about the timing and duration of the expected response. Due to the stricter nature of this model, it is more conservative and may not correctly model the HRF for our region of interest (Calhoun et al., 2004). Paired samples t-tests were used to test for hemisphere effects of total hippocampi, subregions and subfields across conditions. After discovering there were no significant differences of activation across conditions with strict corrections for multiple comparisons, hemispheres were collapsed together. One-sample t-tests were used to compare activity for the total hippocampus bilaterally versus baseline. To investigate the differential involvement of subfields and subregions, we employed repeatedmeasures ANOVAs. Holm-Bonferroni was used to control for multiple comparisons and FWEcorrected values are reported.

Canonical + Derivatives Analysis

HRF modelling was completed using the classical canonical double-gamma function in addition to time and dispersion derivatives. This is more flexible than the classical canonical HRF, and therefore allows for more variation in timing and duration of the response. This model is less conservative and may provide a better fit of the HRF for our data. We relied on nonparametric methodology to resolve ambiguities produced by multi-parameter BOLD response modelling, which sometimes yields ambiguous BOLD response estimates, difficult to classify as either activation or deactivation (Calhoun et al. 2004). The bootstrap technique (100,000 samples) was used to estimate the standard error when evaluating statistical significance of hippocampal activations relative to the baseline task. If the bootstrap distribution was approximately normal, we

used the standard deviation of the bootstrap distribution to estimate the t-static for a given region of interest. Otherwise, bootstrap percentile intervals were used to estimate p-values. HolmBonferroni correction was employed to control for type I error inflation in all tests when testing for presence of activation relative to the baseline. We controlled for multiple comparisons across all conditions for the total hippocampus (3: symbol, location and both), all subregions (9: head/symbol, head/location, head/both, body/symbol, body/location, body/both, tail/symbol, tail/location, tail/both) and all subfields (9: CA/symbol, CA/location, CA/both, DG/symbol, DG/location, DG/both, SUB/symbol, SUB/location, SUB/both). Only FWE-corrected results are reported in the results section. To compare activations between conditions and between hemispheres we used non-parametric permutation tests. A total of 100,000 within-subject shuffles were generated to estimate amplitude differences within conditions across subregions (3: symbol/head&tail, symbol/body&tail, symbol/head&body; 3: location/head&tail, location/body&tail, location/head&body; 3: both/head&tail, both/body&tail, both/head&body) and subfields (3: symbol/CA&DG, symbol/CA&SUB, symbol/DG&SUB; 3: location/CA&DG, location/CA&SUB, location/DG&SUB; 3: both/CA&DG, both/CA&SUB, both/DG&SUB) under the null hypothesis. Similar to earlier tests, Holm-Bonferroni correction for multiple comparisons was applied and only FWE-corrected results are reported. This approach is not often used in the literature because it requires an extensive programming component and major computations that require the use of a supercomputer. Both of these conditions have to be met to analyze the variance of the signal with randomized models and they are not widely available at this time.

Chapter 3: Results

3.1: Behavioural Results

Behavioural results show that participants performed best during the Symbol condition (95.5%). Performance on the more difficult Location and Both conditions was 79.5% and 78.3% respectively (See Figure 3.1). We used a repeated measures ANOVA to compare accuracy across conditions. There was a significant main effect of condition ($F(2,48) = 26.30, p < 0.001$) where performance on the Symbol condition was higher than on the Location ($p < 0.001$) and Both ($p < 0.001$) conditions. There was no significant difference in performance on the Location versus Both conditions ($p = 1.00$).

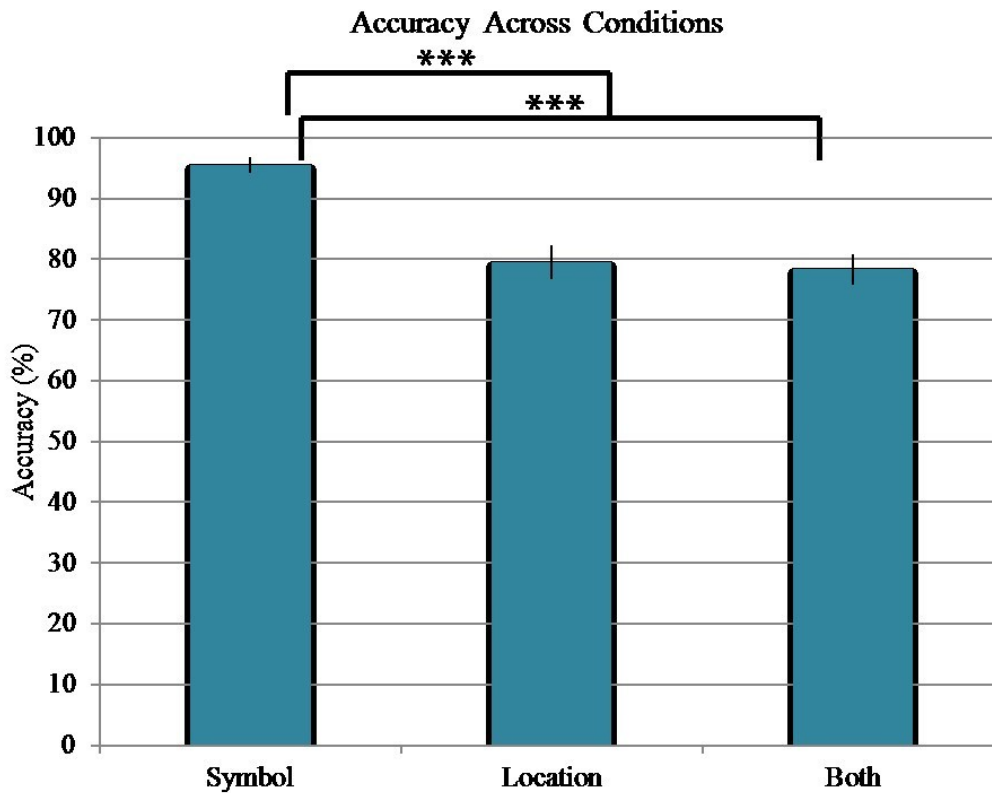


Figure 3.1: Accuracy across conditions displayed in percentage correct. A repeated measures ANOVA demonstrated that participants performed significantly better during the Symbol than during the Location and Both conditions. Error bars indicate standard error.

3.2: Total Hippocampus

Canonical Modelling

Paired samples t-tests corrected for multiple comparisons revealed there were no significant differences in BOLD response between left and right total hippocampi across Symbol ($t(24) = 0.21$, $p = 1.67$) Location ($t(24) = -0.16$, $p = 0.87$) and Both ($t(24) = 2.25$, $p = 0.10$) conditions so they were collapsed together. One sample t-tests showed that the total hippocampus was significantly more active than baseline during encoding of the Symbol ($t(24) = 5.55$, $p = 0.000020$), Location ($t(24) = 6.76$, $p = 0.000003$) and Both ($t(24) = 5.47$, $p = 0.000013$) conditions (See Figure 3.2). A repeated measures ANOVA with hemisphere and condition as factors was employed to assess differential activity of total hippocampi across conditions. No significant main effects or interactions were observed.

Canonical + Derivatives Modelling

There were no laterality effects for the total hippocampus across Symbol ($p = 0.66$), Location ($p = 0.93$) and Both ($p = 0.96$) conditions using a t-test so left and right total hippocampi were collapsed together. The total hippocampus was significantly more active than baseline for encoding of the Symbol, ($t(24) = 4.45$, $p = 0.0005$) Location ($t(24) = 3.13$, $p = 0.0046$) and Both ($t(24) = 3.83$, $p = 0.0016$) conditions (See Figure 3.3). No differences were observed when we compared the total hippocampal response across different encoding conditions (Symbol vs Location: $p = 0.32$; Location vs Both: $p = 0.53$; Symbol vs Both: $p = 0.72$).

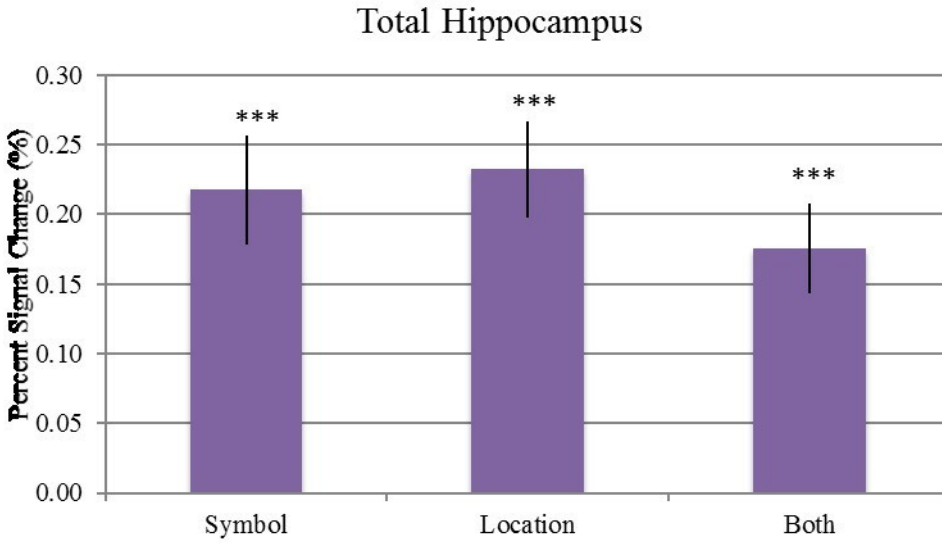


Figure 3.2: Activation for the total hippocampus across conditions using canonical modelling and one-sample t-tests comparing activity relative to baseline. Error bars indicate standard error. (* $p < 0.05$, ** $p < 0.01$, *** $p < 0.001$)

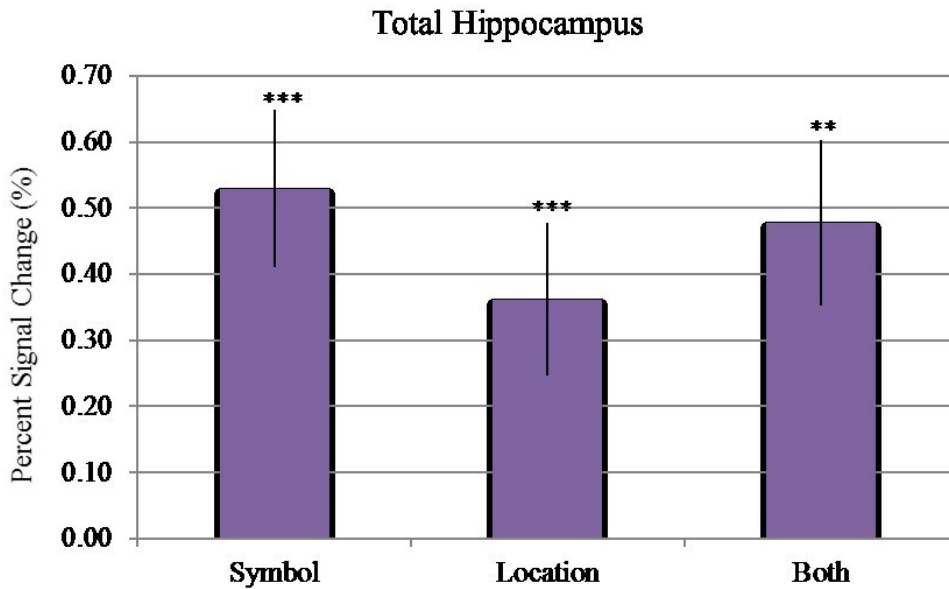


Figure 3.3: Activation for the total hippocampus across conditions using canonical and derivatives modelling and onesample t-tests comparing activity relative to baseline. Error bars indicate standard error. (* $p < 0.05$, ** $p < 0.01$, *** $p < 0.001$)

3.3: Subregions

Canonical Modelling

Paired samples t-tests revealed no significant differences in BOLD signal between hemispheres for the hippocampal head, body and tail subregions during encoding of the Symbol, Location and Both conditions after Holm-Bonferroni correction for multiple comparisons. Therefore, hemispheres were collapsed together for one-sample t-tests to assess activity relative to baseline. One sample t-tests showed that the hippocampal head, body and tail were significantly more active than baseline during encoding of the Symbol (Head: $t(24) = 3.40$, $p = 0.0093$; Body: $t(24) = 4.72$, $p = 0.0006$; Tail: $t(24) = 6.06$, $p = 0.00003$), Location (Head: $t(24) = 4.58$, $p = 0.00007$; Body: $t(24) = 4.85$, $p = 0.00005$; Tail: $t(24) = 3.27$, $p = 0.0098$) and Both (Head: $t(24) = 3.21$, $p = 0.0075$; Body: $t(24) = 3.85$, $p = 0.0039$; Tail: $t(24) = 2.19$, $p = 0.039$) conditions after corrections for multiple comparisons across subregions and conditions (See Figure 3.4).

A repeated measures ANOVA (including hemisphere, subregion and condition as factors) was employed to assess functional heterogeneity of subregions. No significant main effects or interactions were observed. There were trends observed for hemisphere by condition ($F(2,48) = 2.70$, $MSE = 0.31$, $p = 0.078$) and hemisphere by subregion by condition ($F(4,96) = 2.15$, $MSE = 0.13$, $p = 0.080$) interactions.

Canonical + Derivatives Modelling

No laterality effects were observed in the head, body or tail across Symbol, Location and Both conditions (Head/Symbol: $p = 0.80$; Head/Location: $p = 0.41$; Head/Both: $p = 0.52$; Body/Symbol: $p = 0.90$; Body/Location: $p = 0.17$; Body/Both: $p = 0.24$; Tail/Symbol: $p = 0.83$;

Tail/Location: $p = 0.22$; Tail/Both: $p = 0.63$). Therefore we collapsed left and right hippocampal subregions for further analysis.

All subregions were significantly active versus baseline across all conditions of our task (See Figure 3.5). The hippocampal head was significantly active versus baseline for the Symbol, ($t(24) = 4.47$, $p = 0.0013$) Location ($t(24) = 3.05$, $p = 0.0223$) and Both ($p = 0.0206$) conditions. The hippocampal body was significantly active versus baseline for the Symbol ($t(24) = 3.61$ $p = 0.0070$), Location ($t(24) = 3.02$, $p = 0.0177$) and Both ($t(24) = 4.12$, $p = 0.0023$) conditions. The hippocampal tail was significantly active versus baseline for the Symbol ($t(24) = 4.69$, $p = 0.0008$), Location ($t(24) = 4.47$, $p = 0.0011$) and Both ($t(24) = 2.91$, $p = 0.0040$) conditions.

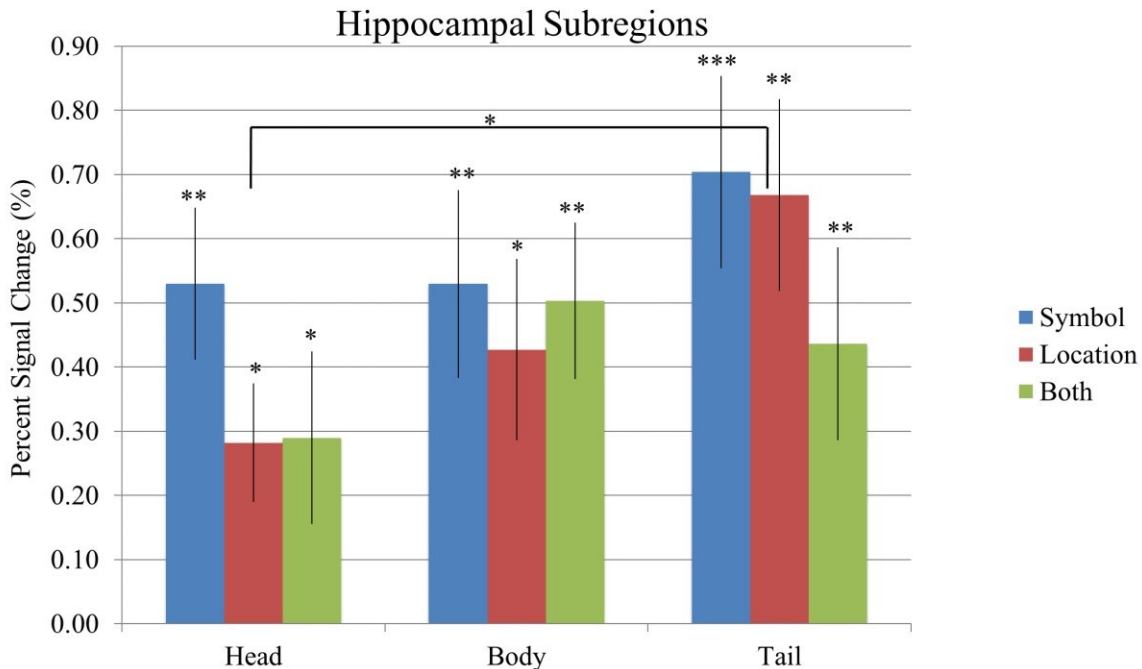


Figure 3.4: Percent signal change activity for subregions (head, body & tail) across conditions using canonical modelling and one-sample t-tests comparing activity relative to baseline. Error bars indicate standard error. (* $p < 0.05$, ** $p < 0.01$, *** $p < 0.001$)

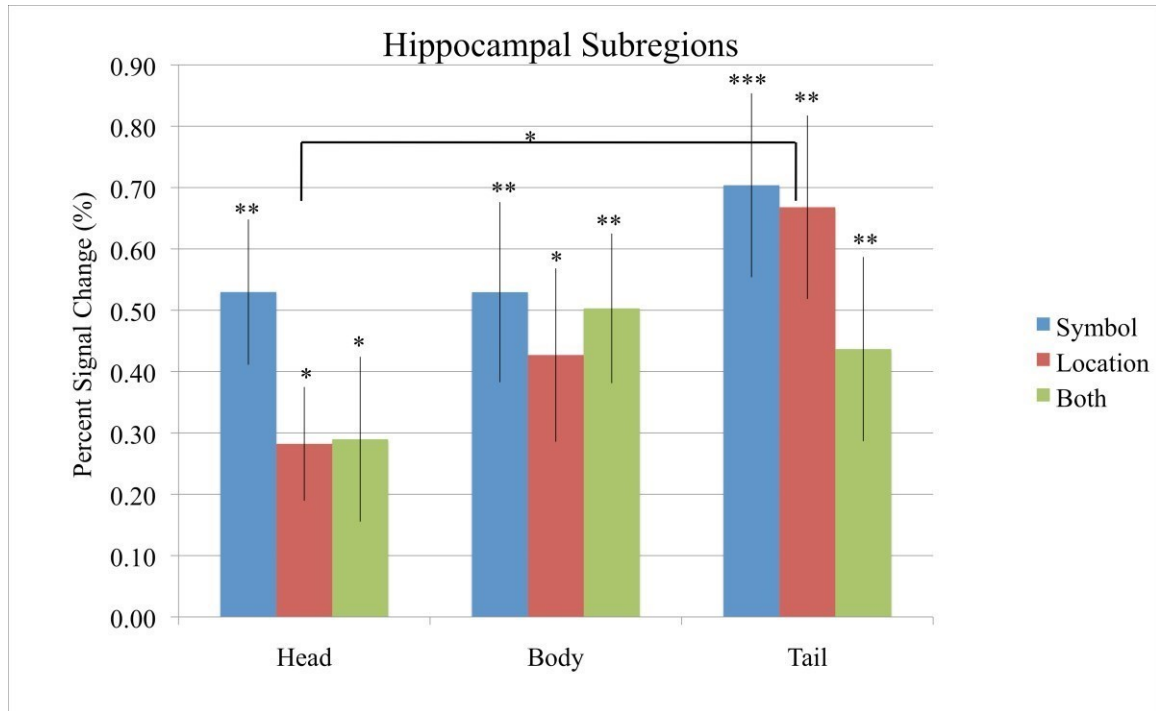


Figure 3.5: Percent signal change activity for subregions (head, body & tail) across conditions using canonical and derivatives modelling and one-sample t-tests comparing activity relative to baseline. Error bars indicate standard error. (* $p < 0.05$, ** $p < 0.01$, *** $p < 0.001$)

Next, we examined whether there were differences in activity across subregions within a condition. There was a significant difference between activation in the head vs tail for the Location condition ($p = 0.047$), where activation in the tail was significantly higher than in the head. No significant difference existed between the head and body ($p = 0.36$) or body and tail ($p = 0.31$) for the Location condition. No differences were observed across subregions for the Symbol (head vs body: $p = 1.0$; body vs tail: $p = 0.27$; head vs tail: $p = 0.22$) or Both conditions (head vs body: $p = 0.27$; body vs tail: $p = 0.72$; head vs tail: $p = 0.54$). Next we compared activation within a subregion across conditions. No differences were observed across conditions within the head (Symbol vs Location: $p = 0.16$; Location vs Both: $p = 0.96$; Symbol vs Both: $p = 0.24$) body (Symbol vs Location: $p = 0.60$; Location vs Both: $p = 0.70$; Symbol vs Both: $p = 0.89$) or tail (Symbol vs Location: $p = 0.88$; Location vs Both: $p = 0.39$; Symbol vs Both: $p = 0.15$).

3.4: Subfields

Canonical Modelling

Paired samples t-tests corrected for multiple comparisons revealed no significant difference between hemispheres after corrections for multiple comparisons across subfields and conditions, so hemispheres were collapsed together for one-sample t-tests to assess activity relative to baseline. One sample t-tests showed that the CA1-3 and DG were significantly active relative baseline during encoding of the Symbol (CA1-3: $t(24) = 4.76$, $p = 0.00039$; DG: $t(24) = 6.34$, $p = 0.000009$), Location (CA1-3: $t(24) = 5.00$, $p = 0.00025$; DG: $t(24) = 4.61$, $p = 0.00045$) and Both (CA1-3: $t(24) = 2.93$, $p = 0.015$; DG: $t(24) = 6.45$, $p = 0.000008$) conditions after corrections for multiple comparisons across subfields and conditions (See Figure 3.9). The Sub was significantly active relative to baseline for the Location ($t(24) = 5.73$, $p = 0.000049$) and Both ($t(24) = 3.93$, $p = 0.0019$) conditions. Sub activation for the Symbol condition ($t(24) = 1.81$, $p = 0.083$) was not significant relative to baseline, but reflected a trend.

To investigate functional heterogeneity of hippocampal subfield activity we completed a repeated measures ANOVA with hemisphere, subfield and condition as factors and post-hoc Bonferroni correction. We observed a significant main effect of subfield ($F(2,48) = 5.18$, $MSE = 0.52$, $p = 0.0092$), where the DG was significantly more active than the CA1-3 across conditions ($p = 0.0007$) (See Figure 3.6). We also observed a significant interaction of hemisphere by subfield ($F(2,48) = 4.51$, $MSE = 0.20$, $p = 0.016$) (See Figure 3.7) and subfield by condition ($F(4,96) = 3.36$, $MSE = 0.19$, $p = 0.013$) (See Figure 3.8). The hemisphere by subfield interaction was followed up using paired samples t-tests for subfields (averaged across conditions) between hemispheres. Results showed CA1-3 activity averaged across all conditions was similar for left and

right hemispheres ($t(24) = -0.22, p = 0.85$), while DG ($t(24) = 2.17, p = 0.040$) and Sub ($t(24) = 2.21, p = 0.037$) activity differed across hemispheres. The subfield by condition interaction was followed up using repeated measures ANOVAs for each condition, with subfields as factors. Results showed that DG activity was greater than CA1-3 ($p = 0.0028$) and Sub ($p = 0.013$) activity for the Symbol condition, DG activity was greater than CA1-3 ($p = 0.0006$) activity for the Both condition, and subfield activity did not differ for the Location condition.

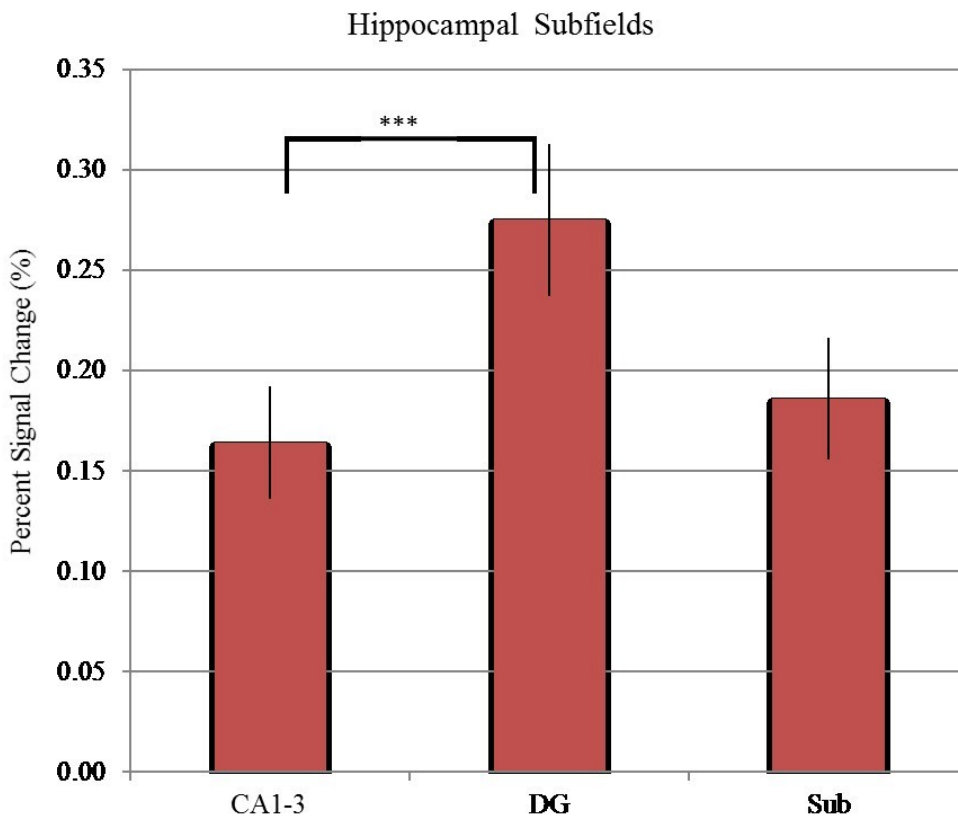


Figure 3.6: Percent signal change activity for subfields (CA1-3, DG & SUB) collapsed across conditions and hemispheres using canonical modelling. A repeated measures ANOVA revealed a main effect of subfield where the DG is significantly more active than the CA1-3. (***) $p < 0.001$

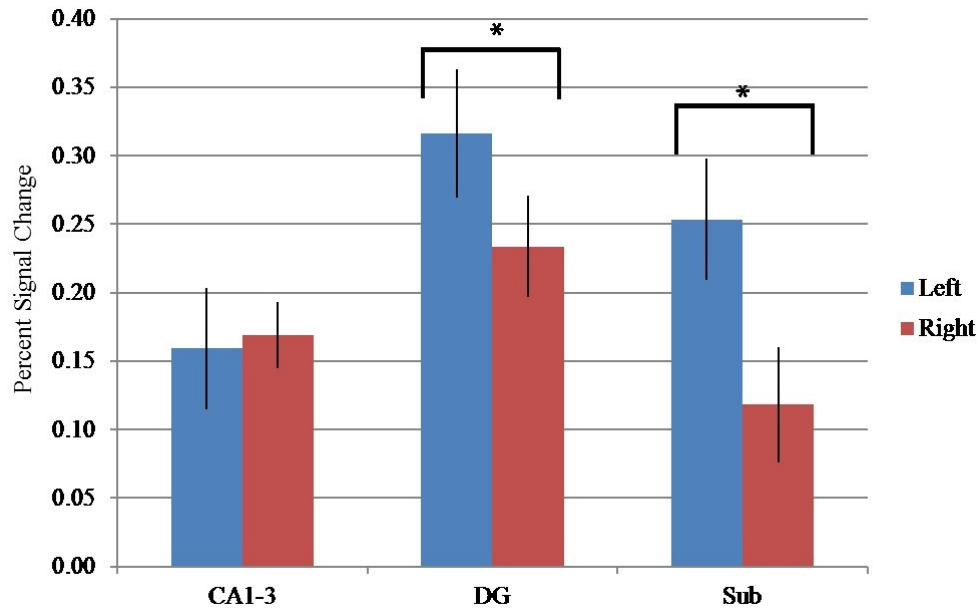


Figure 3.7: Percent signal change activity of subfields (CA1-3, DG & Sub) averaged across conditions. A repeated measures ANOVA revealed a significant Hemisphere by Subfield interaction, where CA1-3 activity was similar for left and right hemispheres, but DG ($p = 0.040$) and Sub ($p = 0.037$) activity was significantly different in left and right hemispheres.

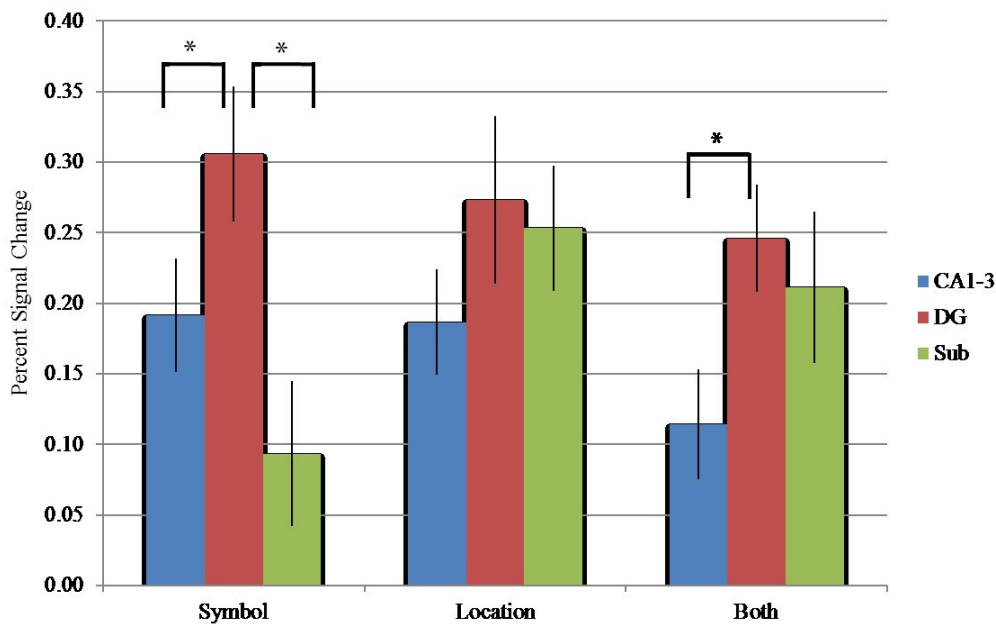


Figure 3.8: Percent signal change activity for subfields within conditions (collapsed across hemispheres). A repeated measures ANOVA revealed a significant Condition by Subfield interaction, where DG activity was significantly larger than CA1-3 ($p = 0.0028$) and Sub ($p = 0.013$) during encoding of the Symbol condition, and DG activity was significantly larger than CA1-3 ($p = 0.0006$) during encoding of the Both condition.

Canonical + Derivatives Modelling

Since we did not observe laterality effects in the CA1-3, DG or Sub across Symbol, Location and Both conditions (CA1-3/Symbol: $p = 0.75$; CA1-3/Location: $p = 0.58$; CA13/Both: $p = 0.51$; DG/Symbol: $p = 0.49$; DG/Location: $p = 0.41$; DG/Both: $p = 0.51$; Sub/Symbol: $p = 0.23$; Sub/Location: $p = 0.75$; Sub/Both: $p = 0.52$) so we collapsed left and right hippocampal subfields together.

All subfields were significantly more active than baseline across all conditions of our task (See Figure 3.10). The CA1-3 subfield was significantly active relative to baseline during encoding of the Symbol ($t(24) = 3.92$, $p = 0.0051$) Location ($t(24) = 3.86$, $p = 0.0045$) and Both ($t(24) = 3.15$, $p = 0.013$) conditions. The DG subfield was significantly more active than baseline during encoding of the Symbol ($t(24) = 3.89$, $p = 0.0048$), Location ($t(24) = 3.82$, $p = 0.0042$) and Both ($p = 0.00004$) conditions. The Sub subfield was significantly more active than baseline during encoding of the Symbol ($t(24) = 3.03$, $p = 0.0116$), location ($t(24) = 2.99$, $p = 0.0063$) and both ($t(24) = 3.74$, $p = 0.0040$) conditions.

Next, we examined whether there were differences in activity across subfields within Symbol, Location and Both conditions. There were no significant differences across subfields within Symbol (CA1-3vs DG: $p = 0.67$; DG vs Sub: $p = 0.27$; CA1-3vs Sub: $p = 0.18$), Location (CA1-3vs DG: $p = 0.38$; DG vs Sub: $p = 0.91$; CA1-3vs Sub: $p = 0.46$) or Both (CA1-3vs DG: $p = 0.22$; DG vs Sub: $p = 0.61$; CA1-3vs Sub: $p = 0.20$) conditions. Next we compared activation within CA, DG and Sub across conditions. No differences were observed within CA1-3(Symbol vs

Location: $p = 0.36$; Location vs Both: $p = 0.68$; Symbol vs Both: $p = 0.26$), DG (Symbol vs Location: $p = 0.83$; Location vs Both: $p = 0.64$; Symbol vs Both: $p = 0.56$) or Sub (Symbol vs Location: $p = 0.48$; Location vs Both: $p = 0.94$; Symbol vs Both: $p = 0.30$) across conditions.

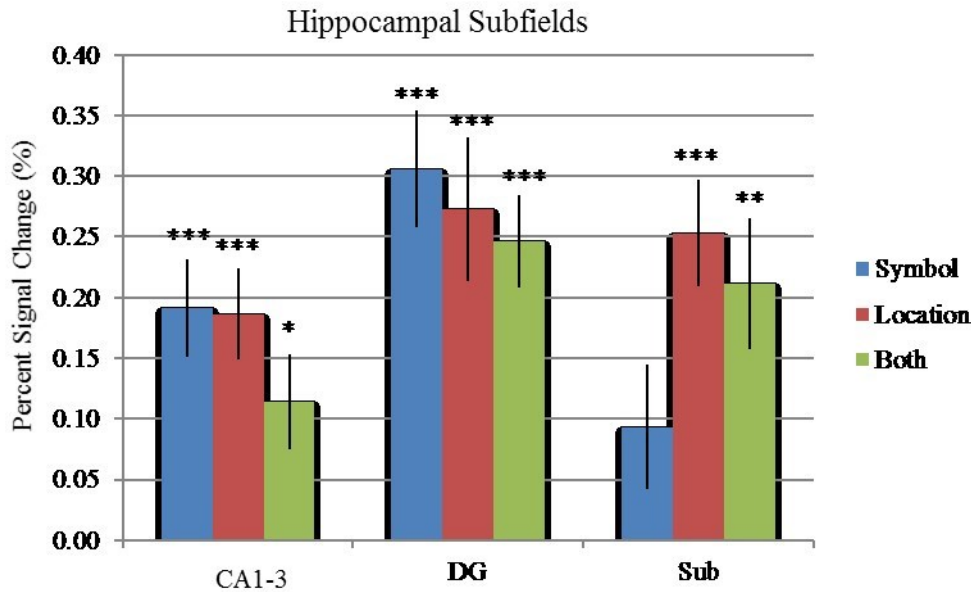


Figure 3.9: Percent signal change activity for subfields (CA1-3, DG & SUB) across conditions using canonical modelling and one-sample t-tests comparing activity relative to baseline. Error bars indicate standard error. (* $p < 0.05$, ** $p < 0.01$, *** $p < 0.001$)

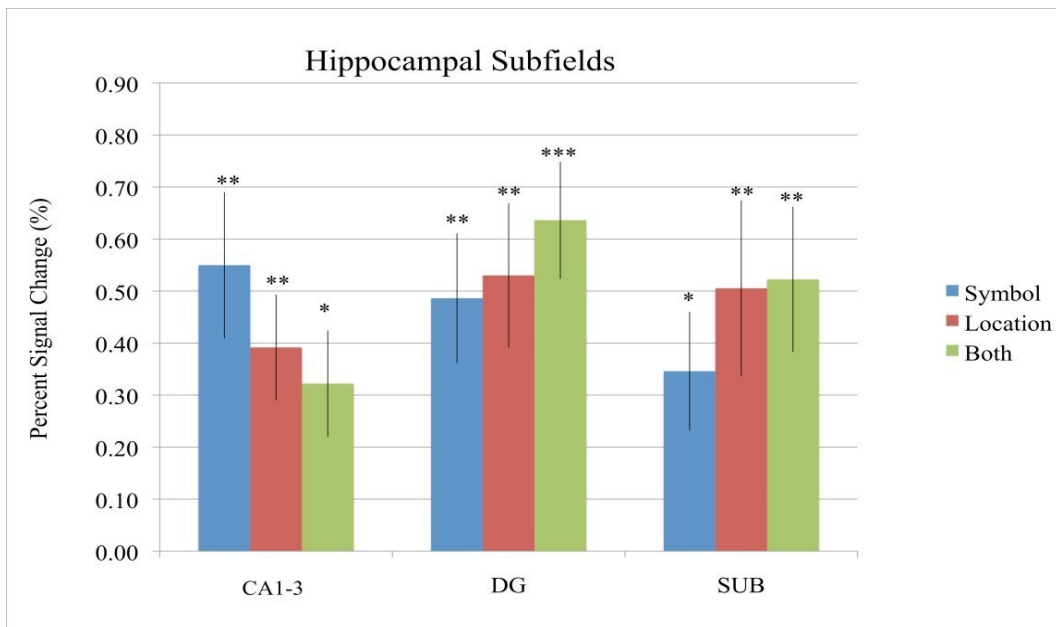


Figure 3.10: Percent signal change activity for subfields (CA1-3, DG & SUB) across conditions using canonical and derivatives modelling and one-sample t-tests comparing activity relative to baseline. Error bars indicate standard error. (* $p < 0.05$, ** $p < 0.01$, *** $p < 0.001$)

Chapter 4: Discussion

Using high-resolution fMRI, an adaptation of the Wechsler Memory Scale Designs Subtest (2009) and two different methods of HRF modelling we demonstrated that the entire hippocampus was active bilaterally during the encoding of content, spatial and associative episodic memories (Symbol, Location and Both conditions respectively). To gain a better understanding of how the hippocampus encodes memories we measured activity across subfields and subregions. We found that all subfields and subregions were significantly active for the encoding of Symbol, Location and Both conditions of our task.

The classical canonical HRF modelling and canonical with time and dispersion derivatives HRF modelling varied in the number of betas they created and the flexibility of the model. The classical canonical HRF (double gamma function) used one set of betas, and used a more strict method of determining the shape of the HRF that was accepted as activity. This model does not accurately account for waves that peak later than anticipated, or that last for a longer than anticipated duration (Calhoun et al., 2004) which may occur in our data when participants view the encoding stimuli over a duration of 10 seconds. The canonical with time and dispersion derivatives HRF model used 3 sets of betas, and allowed the double gamma function in addition to the time and dispersion wave forms to be combined which created a more flexible model. The waves that were accepted as activity did not have to display the typical canonical response in order to contribute to the overall values measured. Therefore, the canonical with time and dispersion derivatives model provided a better fit of the HRF function to our data.

The Canonical model showed that when averaged across all conditions the DG was more active than the CA1-3, and that CA1-3 activity was similar across hemispheres while DG and Sub

activity differed. The lack of difference in hippocampal activity observed across hemispheres may be due to hippocampal commissure connectivity. Previous literature on the rat hippocampus has shown that the hippocampal commissure connects the CA between hemispheres, but not the DG or Sub (Hamilton, 1976). The DG was more active than CA1-3 and Sub during the Symbol condition, and more active than CA1-3 during the Both condition. The Canonical + Derivatives model showed the hippocampal tail was significantly more active than the hippocampal head for the encoding of the Location condition. All other differences were not statistically significant, but may reflect gradients in activation or more subtle differences that may or may not become significant with more power.

4.1 Comparison Canonical & Canonical + Derivative Results

The results observed using the Canonical model and using the Canonical + Derivatives model were similar, but some differences do exist. For a summary of differences in findings, see Table 4.1.

Results for the total hippocampus were similar for the Canonical and Canonical + Derivatives analyses. No hemisphere effects were observed, and the total hippocampus was active relative to baseline across all conditions.

Subregion results were similar for the Canonical and Canonical + Derivatives analyses, but there were also some differences. No hemisphere effects were observed, and all subregions were active relative to baseline across all conditions. The Canonical repeated measures ANOVA showed no significant interactions or effects, but trends of Hemisphere by Condition and Hemisphere by Condition by Subregion. Using the Canonical + Derivatives T-Tests we found a significant difference between the Head and Tail during the Location condition. It is possible that the

Canonical + Derivatives model provided a better fit for the HRF and was able to better assess differences across subregions.

Subfield results were similar for the Canonical and Canonical + Derivatives analyses, but there were some differences. No hemisphere effects were observed, and all subfields were active relative to baseline across all conditions except for the Sub during the Symbol condition using the Canonical Model (which showed a trend). The Canonical repeated measures ANOVA found a significant main effect of subregion, and significant interactions of Hemisphere by Subfield and Subfield by Condition. The Canonical + Derivatives T-Tests did not find any significant differences between the Subfields across conditions. It appears as though the Canonical Model found differences that were not observed using the Canonical + Derivatives bootstrapping methods.

	Canonical + Derivatives: Bootstrapping, Resampling & T-Tests	Canonical: ANOVAs & T-Tests
Total Hippocampus	No difference between hemispheres before correction for multiple comparisons.	No difference between hemispheres after correction for multiple comparisons.
	(Combined hemispheres) Significantly active versus baseline across all conditions	(Combined hemispheres) Significantly active versus baseline across all conditions
	T-Tests show no difference in activity between conditions.	ANOVA shows no difference in activity between conditions.
Subregions	No difference between hemispheres before correction for multiple comparisons.	Difference between hemispheres for Body_Both after correction for multiple comparisons within subregion (*3). If controlled for multiple comparisons across subregions and conditions (*9), difference would not survive.
	(Combined hemispheres) All significantly active versus baseline after correction for multiple comparisons	(Combined hemispheres) All significantly active versus baseline after correction for multiple comparisons within subregions (*3) and across subregions and conditions (*9)
	T-Tests show no significant difference in activity between subregions and conditions.	ANOVA shows no significant effects or interactions, but does show trends.

	N/A	ANOVA Trends: Hemisphere X Condition (p=0.078) Hemisphere X Subregion X Condition (p=0.080)
Subfields	No difference between hemispheres before correction for multiple comparisons.	Difference between hemispheres for DG_Both & Sub_Both after correction for multiple
		comparisons within subfield (*3). If controlled for multiple comparisons across subfields and conditions (*9), differences do not survive.
	(Combined hemispheres) All significantly active versus baseline after correction for multiple comparisons.	(Combined hemispheres) All significantly active versus baseline after correction for multiple comparisons (*9) EXCEPT SUB_Symbol (p=0.083)
	T-Tests show no significant difference in activity between subfields and conditions.	ANOVA shows significant main effect and 2 significant interactions
	N/A	<i>Main effect of Subfield</i> (p=0.009)
	N/A	<i>Significant interaction of Hemisphere X Subfield</i> (p=0.016) and Subfield X Condition (p=0.013)

Table 4.1: Summary of differences observed between Canonical and Canonical + Derivative HRF Modelling

4.2: Models of Hippocampal Structure & Function

The purpose of the current study was to investigate how hippocampal subregions and subfields are involved in the encoding of episodic memory. We wanted to know whether the hippocampus works as a single unit, in discrete sections or in anatomically separate sections that are functionally involved.

The first model of hippocampal function states that the hippocampus functions as separate independent units. It is based on the lamellar hypothesis by Anderson et al. (1971) where stimulation of the perforant pathway resulted in activation that spread across the hippocampus transversely (across subfields) and Bliss and Lomo (1973)'s studies that found evidence of longterm potentiation across subfields. This theory suggests the hippocampus is made up of lamellae with independent circuits across its length (Small et al., 2002). Our results suggest that the entire hippocampus was engaged for our task, and does not provide support for this theory.

The second model of hippocampal function states the hippocampus works as a single functional unit. In Amaral and Witter (1989)'s study they used anterograde and retrograde tracers in a rodent hippocampus. The tracers travelled across the length of the hippocampus suggesting it functioned as a single unit. In Pare et al. (1994)'s electrophysiology study they stimulated entorhinal neurons of a rat. The stimulation resulted activation that spread across the entire length of the hippocampus. This theory suggests the hippocampus functions as a single unit regardless of where cortical input enters the hippocampus and disregards the existence of anterior-posterior subregion specification (Small et al., 2002). Our results provide partial indirect support for this theory as all subfields and subregions are active relative to baseline across all conditions of our task. However for the spatial condition of the memory task, there was a significant difference between the hippocampal head and tail. In addition, the DG was more active than CA1-3 and Sub

during the Symbol condition, and more active than the CA1-3 during the Both condition. These results do not completely agree with the theory that the hippocampus functions as a single unit.

The third model of hippocampal function states that the hippocampus is made up of functionally segregated but interconnected subregions. Using a memory task for faces, names, and face-name pairs Small et al. (2002) assessed this theory of hippocampal function in humans using fMRI. A gradient in activation was observed where when participants heard names the anterior hippocampus was the most active and when they viewed faces the posterior hippocampus was the most active. Retrieval of face-name pairs after a short delay elicited the largest activation in the intermediate hippocampus. If the subregions were functionally separate, activity would be expected in the most anterior and posterior regions as opposed to the intermediate hippocampus. This is support for functionally separate, yet interconnected subregions. In the current study we analyzed hippocampal activation across subregions and subfields during different episodic memory tasks. While the entire hippocampus was engaged for the symbol, location and both conditions, there were regional differences in activity suggesting subfields and subregions may be differentially involved. These variations in activity suggest that while the entire hippocampus is engaged during the task, there are regional differences in how the information is processed. Our results indirectly support the third theory of hippocampal function, which claims differential functional involvement of subregions and subfields.

Many studies have been unable to adequately assess activity across subfields due to limited spatial resolution. The hippocampus is not a large structure at approximately 3300 mm³ (Malykhin et al., 2007). Using typical fMRI the voxel size is usually 4-5 mm before spatial smoothing is applied. This means that cross-sectionally only a few voxels would account for the entire width of the hippocampus. At this resolution, delineation of subfields would not be feasible since the

thickness of CA1-3 and Sub subfields are less than 3 mm. With a strong magnetic field (4.7 T) and small voxel size (1.5 mm x 1.5 mm x 1.4 mm) we were able to acquire high-resolution data to accurately investigate differential activity across subfields.

The CA1-3, DG and Sub were all significantly active relative to baseline during the encoding of the Symbol, Location and Both conditions of our episodic memory task. The polysynaptic pathway of information flow incorporates all subfields of the hippocampus and is associated with episodic memory (Duvernoy, 2013). Although the information flow in this model is much faster than the scale we observe in fMRI, our results are still in agreement with previous literature where all three subfields were engaged in our task. While all subfields were active across all conditions of our task, the activity observed was not equal. The difference between DG and CA1-3 activity averaged across all conditions was statistically significant, where DG activity was larger. This suggests that overall our task engaged the DG more than the CA1-3. When assessing activity within conditions, DG activity was significantly larger than CA1-3 and Sub activity during the Symbol condition, DG activity was significantly larger than CA1-3 during the Both condition and activity did not significantly differ between subfields during the Location condition.

Hippocampal cortical connections vary along the length of the hippocampus, which lends support for their division (Poppenk et al., 2013). The head, body and tail were all significantly active during the Symbol, Location and Both encoding conditions of our episodic memory task. This suggests that all subregions of the hippocampus were engaged across its entire length during our task. During the Location condition of our task there was a significant difference between the head and tail, with the tail eliciting a larger activation. This suggests the hippocampal tail might be more involved in the encoding of spatial memory than the head.

4.3 : Encoding

Previous literature suggests the hippocampus is engaged in the encoding of episodic memory (Poppenk et al., 2013). The question remains in human literature whether the hippocampus as a whole is engaged during encoding or if subregions or subfields are selectively involved. While there is some discrepancy in the field, there are specific subsections of the hippocampus that are thought to be more actively engaged than others during the encoding of an episodic memory task.

An fMRI study by Parsons et al. (2006) studied medial temporal lobe activity along the anterior-posterior gradient while participants encoded auditory or visual stimuli. There was activation in the anterior region regardless of stimulus type for encoding. In addition, a metaanalysis of PET studies by Lepage et al. (1998) found the anterior hippocampus to be more engaged during the encoding and the posterior hippocampus more engaged during retrieval of episodic memory tasks. In the current study we have addressed the question of subregion specificity during encoding. According to our results, all subregions of the hippocampus are actively engaged in the encoding of an episodic memory task. Since we are only assessing activation during the encoding phase we cannot speak to differences between encoding and retrieval. All three hippocampal subregions appear to be active for the encoding of episodic memory for content, spatial and associative memory.

While the evidence for subfield involvement in encoding is less clear, reports of a match/mismatch response or novelty signalling (Reagh et al., 2014) may be related to encoding and retrieval of spatial details. A study by Duncan et al. (2012) observed a match/mismatch signal in the CA1 subfield. Participants studied 30 room layouts along with their associated names. The next day they were re-familiarized with the stimuli prior to entering the MRI scanner. The name of the room would probe participants and they would then be shown a scene with a varying number of

changes to what they had studied. The activity in CA1 was related to the degree of change in the stimuli participants viewed. The authors suggest the CA1 subfield is involved in tracking changes in the environment. This type of cognitive process may reflect some features of encoding. While our delineation of subfields is different, and we analyzed our data in a different way, the current study does provide further support for the CA1-3 subfield's involvement in the encoding of episodic spatial memory.

Our results are not in agreement with previous literature suggesting that hippocampal subfields are differentially involved in a memory (Duncan et al. 2012 ; Reagh et al., 2014). We found that all subfields were significantly active during encoding of all conditions of our memory task. In addition, DG activity was significantly larger than CA1-3 activity across all conditions. Our results may differ due to differences in subfield segmentation, differences in task structure and differences in analysis.

4.4: Spatial Memory

Previous literature has suggested the hippocampus plays an important role in spatial memory (Graham et al., 2010). While previous studies suggest the posterior hippocampus is more engaged than anterior hippocampus there is still no clear agreement in the field. Most fMRI studies of hippocampal subfield activity do not directly address spatial memory in comparison to other kinds of memory (i.e. Duncan et al., 2012; Reagh et al., 2014; Suthana et al., 2015).

Previous literature suggests the posterior hippocampus may be preferentially involved in spatial memory (Lepage et al., 1998), but when damaged the anterior hippocampus may compensate and allow humans or rodents to complete spatial tasks. Moser et al (1995) lesioned rodent hippocampi bilaterally to assess its effect on their spatial learning. The lesions varied from 20% to 100% of total hippocampal volume, from the dorsal or ventral ends. When the ventral

(anterior) hippocampus was not intact, and only 26% of the dorsal (posterior) hippocampus was still intact animals were still able to navigate effectively through a watermaze task. When the dorsal hippocampus was not intact and as much as 60% of the ventral (anterior) hippocampus remained intact the animals exhibited impairment in their ability to complete the task.

Our results suggest the entire hippocampus was engaged during a spatial task, as all subregions were significantly active relative to baseline during the encoding of our spatial episodic memory task. While all regions were active, there was a significant difference between the hippocampal head and tail where hippocampal tail activity was larger. The activity observed across subregions for our study suggests there is a gradient in activation where the posterior hippocampus (hippocampal tail) is most active for our spatial task, followed by the intermediate hippocampus (hippocampal body) and then the anterior hippocampus (hippocampal head). This is in line with previous literature and adds to human studies confirming the posterior hippocampus' involvement in spatial memory.

Previous work in our lab (Travis et al. 2014) found that performance on the Wechsler Memory Scale (2009) was associated with subfield volumes. While visual content memory was associated with only the CA1-3 volume, visual spatial memory was associated with DG and CA13 volume. This suggests both regions may be related to successful spatial encoding and retrieval. The current study has confirmed DG and CA1-3 subfields are actively engaged during the encoding of spatial episodic memory, and also the Sub. Our current findings do not support differential involvement of subfields for spatial memory. While all subfields were significantly active relative to baseline for the encoding of the Location condition, it was the only condition where differences in hippocampal subfield activity were not observed. The hippocampus is known to be active for spatial memory and it appears as though all subfields contribute to this process.

4.5 : Limitations & Future Directions

Our task is designed using abstract symbols, which varies from the traditional everyday objects, words, familiar faces or room layouts that are often employed in hippocampal memory tasks (Spaniol et al., 2009). Initially, we anticipated the abstract images would make it difficult for participants to relate to the stimuli. However, after assessing participant descriptions of memory strategies it appears that participants made connections to these abstract symbols (i.e. “this symbol looks like a stethoscope”). Participants related the abstract symbols to previous experience, which may have resulted in participants forming strong cortical connections for these memories because of the associative process they were engaging in. This may account for the robust activity observed across the entire hippocampus during the Symbol condition.

Some limitations of our study exist as limitations across the field of fMRI. Using our 4.7T system we were able to acquire data with voxel sizes of 1.5 mm x 1.5 mm x 1.5 mm and a TR of 2.5 seconds. These parameters are good for the field, but limit us to inferring activity at 2.5 second intervals, and 1.5 mm isotropic resolution. While our masks were all created in structural space with 0.52 x 0.68 x 1 mm³ resolution, they had to be transferred into 1.5 mm space, taking away some of the specificity created in the original tracings. There is also some discrepancy in the field as to how to delineate the subfields of the hippocampus which means that our CA1-3 region may not be a perfect match for the CA2-3 region in another study, etc. This means that when taking results from other studies and applying them to our project caution must be taken as the regions may not have absolute overlap. However, this is an issue with all hippocampal fMRI research and there is a committee developed to address this issue and come up with a harmonized protocol to improve this problem (Yushkevitch et al., 2015). Future work should keep these discrepancies in

subfield delineation in mind and stay up to date on the hippocampal segmentation summit's progress.

Due to high accuracy during our task, we are unable to compare correct and incorrect trials to look at subsequent memory effects. Future work could modify sections of the task to increase difficulty by adding more items to remember and allow for this type of analysis. We were able to detect a significant difference in activation during all conditions of our task versus baseline, the differences observed across subregions and subfields, and across conditions were limited. The next step in our analysis will be to analyze activity in the anterior (head) versus posterior (body and tail) hippocampus. Future research could focus on one condition of our task and acquire more data to give more power in analysis. This could confirm whether the patterns we see in the current study are indicative of strong differences in subregion and subfield activity or not, and could provide stronger support for the use of classical Canonical or Canonical + Derivative modelling.

4.6: Summary

With the use of high-resolution fMRI, adaptation of a standard clinical episodic memory task based on Wechsler Memory Scale (2009), and an advanced manual segmentation protocol for hippocampal subfields and subregions we investigated how the hippocampus encodes episodic memory. Using classical Canonical modelling and Canonical with derivative modelling we found that the total hippocampus in addition to all subfields and all subregions were significantly active relative to baseline during the encoding phase of the Symbol, Location and Both conditions of our task. This suggests the hippocampus as a whole and its smaller parts are engaged in the encoding of episodic content, spatial and associative memory. The Canonical + Derivatives model showed the hippocampal tail was more active than the hippocampal head for the location condition of our task, providing support for the posterior hippocampus' preferential involvement in spatial memory.

The Canonical model showed that when averaged across all conditions the DG was more active than CA1-3, and that CA1-3 activity was similar across hemispheres while DG and Sub activity differed. The DG was more active than CA1-3 and Sub during the Symbol condition, and more active than CA1-3 during the Both condition. Our use of two different HRF models and analysis procedures showed that the way you analyze your data could modify your results. Some approaches are more sensitive than others for assessing differential activity. Our study contributes to current knowledge of how the human hippocampus encodes episodic memories.

References

- Aksoy-Aksel, A & Manaham-Vaughan, D. (2013). The temporoammonic input to the hippocampal CA1 region displays distinctly different synaptic plasticity compared to the Schaffer collateral input in vivo: significance for synaptic information processing. *Frontiers in Synaptic Neuroscience*. 5, 1-12.
- Amaral, D.G., Witter, M.P. (1989). The three-dimensional organization of the hippocampal formation: a review of anatomical data. *Neuroscience*. 31, 571-591.
- Anderson, P, Bliss, T.V., Skrede, K.K. (1971). Lamellar organization of hippocampal pathways. *Experimental Brain Research*. 13, 222-238.
- Baumann, O. & Mattingley, J. B. (2013). Dissociable representations of environmental size and complexity in the human hippocampus. *Journal of Neuroscience*. 33, 10526–10533.
- Birn, R.M., Diamond, J.B., Smith, M.A. & Bandettini, P.A. (2006). Separating respiratoryvariation-related fluctuations from neuronal-activity-related fluctuations in fMRI. *Neuroimage*. 31, 1536-1548.
- Birn, R.M., Smith, M.A., Jones, T.B. & Bandettini, P.A. (2008). The respiration response function: The temporal dynamics of fMRI signal fluctuations related to changes in respiration. *Neuroimage*. 40, 644-654.
- Bliss, T.V., Lomo, T. (1973). Long-lasting potentiation of synaptic transmission in the dentate area of the anaesthetized rabbit following stimulation of the perforant path. *The Journal of Physiology*. 232, 331-356.

Calhoun, V.D., Stevens, M.C., Pearlson, G.D. & Kiehl, K.A. (2004). fMRI analysis with the general linear model: removal of latency-induced amplitude bias by incorporation of hemodynamic derivative terms. *Neuroimage*. 22, 252–257.

Chang, C., Cunningham, J.P. & Glover, G.H. (2009) Influence of heart rate on the BOLD signal: The cardiac response function. *Neuroimage*. 44, 857-869.

De Vanssay-Maigne, A. Noulhiane, M., Devauchelle, A.D., Rodrigo, S., Baudoin-Chial, S., Meder, J.F., Oppenheim, C., Chiron, C. & Chassoux, F. (2011). Modulation of encoding and retrieval by recollection and familiarity: Mapping the medial temporal lobe networks. *Neuroimage*. 58, 11311138.

Devonshire, I.M., Papadakis, N.G., Port, M., Berwick, J., Kennerly, A.J., Mayhew, J.E.W., Overton, P.G., 2012. Neurovascular coupling is brain region-dependent. *Neuroimage* 59, 1997–2006.

Duncan K., Ketz N., Inati S.J. & Davachi L. (2012). Evidence for area CA1 as a match/mismatch detector: a high-resolution fMRI study of the human hippocampus. *Hippocampus*. 22(3), 389398.

Duvernoy, H.M. (2005). *The human hippocampus: Functional anatomy, vascularization, and serial sections with MRI*. Berlin Heidelberg: Springer-Verlag

Duvernoy, H.M., Cattin, F., Risold, P.Y. (2013). *The human hippocampus: Functional anatomy, vascularization, and serial sections with MRI*. Berlin Heidelberg: Springer-Verlag

Eichenbaum, H. (2001). The hippocampus and declarative memory: cognitive mechanisms and neural codes. *Behavioural Brain Research*. 127(1-2), 199-207.

Glover, G.H., Li, T. & Ress, D. (2000). Image-based method for retrospective correction of physiological motion effects in fMRI: RETROICOR. *Magnetic Resonance in Medicine*. 44, 162167.

Graham, K.S., Barense, M.D. & Lee, A.C.H. (2010). Going beyond LTM in the MTL: A synthesis of neuropsychological and neuroimaging findings on the role of the medial temporal lobe in memory and perception. *Neuropsychologia*. 48, 831-853.

Hamilton, L.W. (1976). *Basic Limbic System Anatomy of the rat*. Heidelberg: Springer-Verlag US

Handwerker, D.A., Ollinger, J.M., D'Esposito, M., 2004. Variation of BOLD hemodynamic responses across subjects and brain regions and their effects on statistical analyses. *Neuroimage* 21, 1639–1651.

Hartley, T., Maguire, E. A., Spiers, H. J. & Burgess, N. (2003). The well-worn route and the path less traveled: distinct neural bases of route following and wayfinding in humans. *Neuron*, 37, 877888.

Hawrylycz, M.J., Lein, E.S., Guillozet-Bongaarts, A.L., Shen, E.H., Ng, L., Miller, J.A., van de Lagemaat, L.N., Smith, K.A., Ebbert, A., Riley, Z.L., Abajian, C., Beckmann, C.F., Bernard, A., Bertagnolli, D., Boe, A.F., Cartagena, P.M., Chakravarty, M.M., Chapin, M., Chong, J., Dalley, R.A., Daly, B.D., Dang, C., Datta, S., Dee, N., Dolbeare, T.A., Faber, V., Feng, D., Fowler, D.R., Goldy, J., Gregor, B.W., Haradon, Z., Haynor, D.R., Hohmann, J.G., Horvath, S., Howard, R.E., Jeromin, A., Jochim, J.M., Kinnunen, M., Lau, C., Lazarz, E.T., Lee, C., Lemon, T.A., Li, L., Li, Y., Morris, J.A., Overly, C.C., Parker, P.D., Parry, S.E., Reding, M., Royall, J.J., Schulkin, J., Sequeira, P.A., Slaughterbeck, C.R., Smith, S.C., Sodt, A.J., Sunkin, S.M., Swanson,

B.E., Vawter, M.P., Williams, D., Wohnoutka, P., Zielke, H.R., Geschwind, D.H., Hof, P.R., Smith, S.M., Koch, C., Grant, S.G., Jones, A.R. (2012). An anatomically comprehensive atlas of the adult human brain transcriptome. *Nature*. 489, 391–399.

Insausti, R. (1993). Comparative anatomy of the entorhinal cortex and hippocampus in mammals. *Hippocampus*. 3, 19–26.

Jeneson, A. & Squire, L.R., (2011). Working memory, long-term memory, and medial temporal lobe function. *Learning & Memory*, 19(1), 15-25.

Leal, S.L., Tighe, S.K., Jones, C.K. & Yassa, M.A. (2014). Pattern separation of emotional information in hippocampal dentate and CA3. *Hippocampus*. 24, 1146-1155.

Lepage, M., Habib, R. & Tulving, E. (1998). Hippocampal PET activations of memory encoding and retrieval: the HIPER model. *Hippocampus*. 8(4), 313-322.

Malykhin, N.V., Lebel, R.M., Coupland, N.J., Wilman, A.H., & Carter, R. (2010). In vivo quantification of hippocampal subfields using 4.7 T fast spin echo imaging.

Neuroimage, 49,1224-30.

Malykhin, N.V., Bouchard, T.P., Ogilvie, C.J., Coupland, N.J., Seres, P., Camicioli, R., (2007).

Three-dimensional volumetric analysis and reconstruction of amygdala and hippocampal head, body and tail. *Psychiatry Research: Neuroimaging*. 155(2), 155–165.

Mayes, A., Montaldi, D. & Migo, E. (2007). Associative memory and the medial temporal lobes.

Trends in Cognitive Sciences. 11(3), 126-135.

Milner B, Corkin S, & Teuber HL. (1968). Further analysis of the hippocampal amnesic syndrome:

14 year follow-up study of H.M. *Neuropsychologia*. 6, 215–34.

- Moser, M.B., Moser, E.I., Forrest, E., Andersen, P. & Morris, R.G.M. (1995). Spatial learning with a minislab in the dorsal hippocampus. *Proceedings of the National Academy of Sciences of the United States*. 92, 9697–9701.
- Nelder, J.A. & Mead, R. (1965). A simplex method for function minimization. *The Computer Journal*. 7, 308–313.
- Neuner, I., Stocker, T., Kellermann, T., Kircher, T., Zilles, K., Schneider, F. & Shah, N.J. (2007). Wechsler memory scale revised edition: Neural correlates of the visual paired associates subtest adapted for fMRI. *Brain Research*. 1177, 66-78.
- Olson IR, Moore KS, Stark M, Chatterjee A. (2006). Visual working memory is impaired when the medial temporal lobe is damaged. *Journal of Cognitive Neuroscience*, 18. 1087–1097. Pare, D., Llinas, R. (1994). Non-lamellar propagation of entorhinal influences in the hippocampal formation: multiple electrode recordings in the isolated guinea pig brain in vitro. *Hippocampus*. 4, 403-409.
- Parsons, M.W., Haut, M.W., Lemieux, S.K., Moran, M.T. & Leach, S.G. (2006). Anterior medial temporal lobe activation during encoding of words: fMRI methods to optimize sensitivity. *Brain and Cognition*. 60(30). 253-261.
- Pernet, C.R., 2014. Misconceptions in the use of the General Linear Model applied to functional MRI: a tutorial for junior neuro-imagers. *Front. Neurosci*. 8, 1.
- Piekema, C. Kessels, R.P.C., Rijpkema, M. & Fernandez, G. (2009). The hippocampus supports encoding of between-domain associations within working memory. *Learning & Memory*. 16, 231234.
- Piekema, C., Rijpkema, M., Fernandez, G. & Kessels, R.P.C. (2010). Dissociating the neural correlates of intra-item and inter-item working-memory binding. *Plos One*. 5(4), 1-8.

- Poppenk, J., Evensmoen, H.R., Moskovitch, M. & Nadel, L. (2013). Long-axis specialization of the human hippocampus. *Trends in Cognitive Neuroscience*. 17(5), 230-240.
- Reagh, Z.M. Watabe, J., Ly, M., Murray, E. & Yassa, M.A. (2014). Dissociated signals in human dentate gyrus and CA3 predict different facets of recognition memory. *Journal of Cognitive Neuroscience*. 34(40), 546-559.
- Sadeh, T., Maril, A. & Goshen-Gottstein, Y. (2012). Encoding-related brain activity dissociates between the recollective processes underlying successful recall and recognition: a subsequentmemory study. *Neuropsychologia*. 50, 2317-24.
- Schultz, H., Sommer, T. & Peters, J. (2012). Direct evidence for domain-sensitive functional subregions in human entorhinal cortex. *The Journal of Neuroscience*. 32(14). 4716-4723.
- Scoville, W.B., & Milner, B. (1957). Loss of recent memory after bilateral hippocampal lesions. *Journal of Neurology, Neurosurgery, and Psychiatry*, 20, 11-21.
- Small, S.A. (2002). The longitudinal axis of the hippocampal formation: Its anatomy, circuitry, and role in cognitive function. *Reviews in the Neurosciences*. 13(2), 183-194.
- Spaniol, J., Davidson, P.S., Kim A.S., Moscovitch, M. & Grady, C.L. (2009). Event-related fMRI studies of episodic encoding and retrieval: meta-analyses using activation likelihood estimation. *Neuropsychologia*. 47, 1765–1779
- Squire, L.R. & Dede, A.J., (2015). Conscious and unconscious memory systems. *Cold Harbor Perspectives in Biology*, 7(3), 1-14.
- Squire L.R., Genzel L., Wixted J.T. & Morris RG. (2015). Memory Consolidation. *Cold Spring Harbor Perspectives in Biology*, 7(8), 1-21.

Squire, L.R. & Zola-Morgan, J.T. (1991). The cognitive neuroscience of human memory since H.M. *Annual Review of Neuroscience*. 34, 259-288.

Squire, L.R. & Zola, S.M. (1996). Structure and function of declarative and nondeclarative memory systems. *Proceedings of the National Academy of Sciences*. 93, 13515-13522.

Strange, B.A., Fletcher, P.C., Henson, R.N.A., Friston, K.J. & Dolan, R.J. (1999). Segregating the functions of human hippocampus. *Proceedings of the National Academy of Sciences*, 96, 4034–4039.

Strange, B.A., Witter, M.P., Lein, E.S. & Moser, E.I. (2014). Functional organization of the hippocampal longitudinal axis. *Nature Reviews Neuroscience*. 15, 655-669.

Stokes, J., Kyle, C. & Ekstrom, A.D. (2015). Complementary roles of human hippocampal subfields in differentiation and integration of spatial context. *Journal of Cognitive Neuroscience*. 27(3), 546-559.

Suthana, N.A., Donix, M., Wozny, D.R., Bazih, A., Jones, M., Heidermann, R.M., Trampel, R., Ekstrom, A.D., Scharf, M., Knolton, B., Turner, R. & Bookheimer, S.Y. (2015). High-resolution 7T fMRI of human hippocampal subfields during associative learning. *Journal of Cognitive Neuroscience*. 27(6), 1194-1206.

Travis, S.G., Huang, Y., Fujiwara, E., Radomski, A., Olsen, F., Carter, R., Seres, P., & Malykhin, N.V. (2014). High field structural MRI reveals specific episodic memory correlates in the subfields of the hippocampus. *Neuropsychologia*, 53. 233-245

Tulving, E. (2002). Episodic memory: From mind to brain. *Annual Review of Psychology*. 53(1), 1-25.

Wechsler, D. (2009). Wechsler Memory Scale-IV administration and scoring manual. San Antonio, TX: Pearson.

Wixted, J.T., Mickes, L. & Squire, L.R. (2010). Measuring recollection and familiarity in the medial temporal lobe. *Hippocampus*. 20(11), 1195-1205.

Yushkevich, P.A., Amaral, R.S.C., Augustinack, J.C, Bender, A.R., Bernstein, J.D., Boccardi, M., Bocchetta, M., Burggren, A.C., Carr, V.A., Chakravarty, M.M., Chetelat, G., Daugherty, A.M., Davachi, L., Ding, S., Ekstrom, A., Geerlings, M.I., Hassan, A., Huang, Y., Iglesias, J.E., La Joie, R., Kerchner, G.A., LaRocque, K.F., Libby, L.A., Malykhin, N., Mueller, S.G., Olsen, R.K., Palombo, D.J., Parekh, M.B., Pluta, J.B., Preston, A.R., Pressner, J.C., Ranganath, C., Raz, N., Schlichting, M.L., Schoemaker, D., Singh, S., Stark, C.E.L., Suthana, N., Tompary, A., Turowski, M.M., Leemput, K.V., Wagner, A.D., Wang, L., Winterburn, J.L., Wisse, L.E.M., Yassa, M.A. & Zeineh, M.M. (2015) Quantitative comparison of 21 protocols for labeling hippocampal subfields and parahippocampal cortical subregions in vivo mri: Towards developing a harmonized segmentation protocol. *Neuroimage*. 111, 526-41.

Zeineh, M.M., Engel, S.A., Thompson, P.M., & Bookheimer, S.Y. (2003). Dynamics of the hippocampus during encoding and retrieval of face–name pairs. *Science*, 299, 577–580.